



Contents lists available at ScienceDirect

Journal of Computational and Applied Mathematics

journal homepage: www.elsevier.com/locate/cam

Numerical integration of a hierarchically size-structured population model with contest competition

α1 L.M. Abia^a, O. Angulo^{b,*}, J.C. López-Marcos^a, M.A. López-Marcos^a

^a Departamento de Matemática Aplicada. Facultad de Ciencias. Universidad de Valladolid. Valladolid, Spain

^b Departamento de Matemática Aplicada. ETS de Ingenieros de Telecomunicación. Universidad de Valladolid. Paseo de Belén, 15 - Campus Miguel Delibes, 47011 Valladolid, Spain

ARTICLE INFO

Article history:

Received 21 June 2013

Received in revised form 9 July 2013

Keywords:

Hierarchically size-structured population models

Numerical integration

Convergence

ABSTRACT

We formulate schemes for the numerical solution to a hierarchically size-structured population model. The schemes are analysed and optimal rates of convergence are derived. Some numerical experiments are also reported to demonstrate the predicted accuracy of the schemes and to show their behaviour to approaching stable steady states.

© 2013 Published by Elsevier B.V.

1. Introduction

The study of population dynamics has evolved from simple unstructured models to fairly sophisticated structured ones. In these, there exists a variable which structures the population into different classes. The most widely used is age, but it is difficult to measure in a large number of species. Physiological characteristics, grouped generically under the name of size, are the alternative to age. These structured population models involve a first-order hyperbolic partial differential equation which represents a conservation law for the population, a boundary condition which reflects the reproduction process and an initial condition given by the initial size-distribution of the population. The evolution of the population is determined by so-called “vital functions” (fertility, mortality and growth rates). Reciprocally, the population also has an influence on such evolution through the vital functions which depend on functionals of the population density, so that the model becomes a nonlinear one. We can find more details about physiologically structured models in [1–4], about their numerical integration we refer to [5,6] and about the computational study of real populations. See, for example, [7–11].

The model we study in this work assumes that the influence of the population on the life-history of individuals is of a contest kind. This means that the individuals in the population do not have the same opportunity in the competition for resources. This kind of model is known as a hierarchical size-structured population one. Here, we study a standard problem. It consists of a nonlinear partial differential equation (the population balance law),

$$u_t + (g(x, B(x, t), t) u)_x = -\mu(x, B(x, t), t) u, \quad x_m < x < x_M, \quad t > 0, \quad (1.1)$$

a nonlinear and nonlocal boundary condition which represents the birth law,

$$g(x_M, B(x_M, t), t) u(x_M, t) = \Gamma(t) + \int_{x_m}^{x_M} \alpha(x, B(x, t), t) u(x, t) dx, \quad t > 0, \quad (1.2)$$

* Corresponding author. Tel.: +34 983 423000X5680; fax: +34 983 423 661.

E-mail addresses: abia@mac.uva.es (L.M. Abia), oscar@mat.uva.es (O. Angulo), lopezmar@mac.uva.es (J.C. López-Marcos), malm@mac.uva.es (M.A. López-Marcos).

and an initial condition,

$$u(x, 0) = \phi(x), \quad x_m \leq x \leq x_M, \quad (1.3)$$

where the nonlocal term $B(x, t)$, is defined by

$$B(x, t) = \int_x^{x_M} \gamma(\sigma) u(\sigma, t) d\sigma, \quad x_m < x < x_M, \quad t > 0. \quad (1.4)$$

The independent variables x and t represent size and time, where x_m and x_M are, respectively, the minimum and maximum value reached by an individual in a given population. The function $u(x, t)$ is the size-specific population density of individuals with size x at time t . We also assume that the size of any individual varies according to the following ordinary differential equation

$$\frac{d}{dt}x(t) = g(x(t), B(x(t), t), t). \quad (1.5)$$

Population dynamics are determined by the growth rate g , the mortality rate μ , the reproduction rate α and the external inflow Γ . These nonnegative vital functions (growth, mortality and reproduction rates) depend on the structuring variable and on the functional $B(x, t)$ used to describe the competition among individuals. In this case, no individual in a class of a smaller size can affect the amount of available resources of an individual larger in size, which is a kind of contest competition. Also, all the functions depend on the time variable in order to take into account environmental changes. We could consider different functionals in the vital functions dependency (g , μ and β). It would increase the complexity of the numerical method description. However, this more general case would not increase the difficulty of the analysis.

This model can be used to describe the dynamics of a size-structured tree population which takes into account the effect of competition for light [12–14]. In this case, the size is given by the diameter at breast height (d.b.h.) and $B(x, t)$ represents the cumulative basal area of trees with a size greater than x and expresses the shading effect under light competition.

From a theoretical point of view, Cushing [15] was the first to study a model like this. It was structured by age and included a more general type of nonlinearity in which the vital rates depended on the number of older and/or younger individuals than itself. However, the approach was limited to vital rates with no explicit age dependence. Later, in [16], Calsina and Saldaña considered a hierarchically size-structured model, but they did not include explicit dependence on size in the vital rates. They obtained the existence, uniqueness, asymptotic behaviour of the solutions and global asymptotic stability of a nontrivial equilibrium. The existence and uniqueness of solutions for an autonomous model which included the explicit dependence on the structured variable were studied by Kraev [17]. And Ackleh and Ito, in [18], proved the existence of measure-valued solutions in a more general setting with less restrictions for the growth rate.

We should point out here that, without other restrictive assumptions, this kind of model cannot be solved analytically. Moreover, when such models include nonlinearities and environmental dependence on the different vital rates, the use of efficient methods that provide a numerical approach is the most suitable mathematical tool for studying the problem and, indeed, is often the only one available. Nevertheless, the numerical approach to these equations has important drawbacks because they are usually nonlinear equations, and the nonlinearities of the PDE and nonlocal boundary condition are caused by nonlocal terms. The model (1.1)–(1.4) was studied in [19], where an implicit first-order finite difference scheme was analysed and its stability and convergence, as well as the existence, uniqueness, and well-posedness (in the L^1 norm) of bounded variation weak solutions for (1.1), were proved. In [20], for the autonomous version of (1.1)–(1.4), Shen et al. proved the convergence of an upwind scheme and another method which were only first-order in time and second-order in size discretization.

In the present paper, we introduce second-order numerical methods for the solution to this nonlinear and nonautonomous model and we also develop the convergence analysis of a general formulation. We carry out the numerical integration of Eqs. (1.1)–(1.4) by means of methods which integrate along the characteristic curves in different settings: the use of all the grid nodes, the use of a grid with a constant number of nodes in every time step by means of a suitable selection, and the use of a more specific selection of grid nodes which allows us to change their number (increasing or diminishing). The integral terms are approximated by means of second-order quadrature rules. We analyse the consistency, stability and convergence properties of a general numerical scheme which covers the situation where the quadrature rule used at a time step is based on nodes obtained by integration along the characteristics with the nodes employed at the previous time step. We also provide numerical experiments to show the accuracy of the schemes and their behaviour in long time integration. These methods could be clearly generalized for other situations like the ones studied in [21]. Also, we would like to point out that the nonautonomous case is important from the biological point of view, as we can see in [22] and the references therein.

Throughout the paper we assume the following regularity conditions on the data functions and the solution to the problem (1.1)–(1.4) which will be integrated in a fixed time interval $[0, T]$:

$$(H1) \quad u \in \mathcal{C}^2([x_m, x_M] \times [0, T]), \quad u(x, t) \geq 0, \quad x \in [x_m, x_M], \quad u(x_M, t) = 0, \quad t \geq 0.$$

$$(H2) \quad \gamma \in \mathcal{C}^2([x_m, x_M]).$$

$$(H3) \quad \Gamma \in \mathcal{C}^1([0, T]).$$

$$(H4) \quad \mu \in \mathcal{C}^2([x_m, x_M] \times D_B \times [0, T]), \text{ is nonnegative.}$$

Table 1

Notation.

Model			
x_m	Minimum size	x_M	Maximum size
g	Growth rate	B	Competition functional
μ	Mortality rate	γ	Weight function
α	Fertility rate	ϕ	Initial density
Γ	external inflow	D_B	Compact neighbourhood
$[0, T]$	Fixed time interval		
Numerical integration			
$x(t; t^*, x^*)$	Characteristic curve	m	Auxiliary rate
$w(t; t^*, x^*)$	Solution along characteristic curve	N	Number of time steps
$J + 1$	Number of initial grid nodes	h	Spatial discretization parameter
k	Time discretization parameter	t_n	Discrete time level
$J_n + 1$	Number of Grid nodes at t_n	X_j^n	Grid node
U_j^n	Numerical Approximation of $u(X_j^n, t_n)$	I_j^n	Numerical approximation to $B(X_j^n, t_n)$
\mathcal{Q}_j	Quadrature rule	$X_j^{n,*}$	Auxiliary node
$U_j^{n,*}$	Auxiliary solution approximation	$I_j^{n,*}$	Auxiliary functional approximation
β	Fixed value in selection strategy (2.20)	λ_n	number of eliminated nodes
Convergence			
H	Set of h values	r	Fixed positive constant
\mathcal{A}_h	Space of approaches	\mathcal{B}_h	Space of residuals
\mathbf{x}_h	Theoretical grid values	\mathbf{u}_h	Theoretical solution values
R, p	Positive constants	Φ_h	Discretization operator
$\mathbf{y}^n, \mathbf{z}^n$	Related to grid values	$q_i^{n,j}$	Quadrature weight
$\mathbf{V}^n, \mathbf{W}^n$	Related to solution values	$\lambda_{ j }^n$	First subgrid subindex greater than j
$\mathbf{Y}^n, \mathbf{Z}^n$	Related to residuals in grid approach	\mathbf{l}_h	Local discretization error
$\mathbf{P}^n, \mathbf{L}^n$	Related to residuals in solution approach	\mathbf{e}_h	Global discretization error

(H5) $\alpha \in \mathcal{C}^2([x_m, x_M] \times D_B \times [0, T])$, is nonnegative.

(H6) $g \in \mathcal{C}^3([x_m, x_M] \times D_B \times [0, T])$, is nonnegative, $g(x_m, z, t) \geq C > 0$, $g(x_M, z, t) = 0$, and $g_z(x, z, t) \leq 0$, $x \in [x_m, x_M]$, $z \in \mathbb{R}$, $t > 0$.

In hypotheses (H4)–(H6), D_B is a compact neighbourhood of

$$\{B(x, t), x_m \leq x \leq x_M, 0 \leq t \leq T\}.$$

The above hypotheses can be based on three possible reasons. First, biological assumptions such as the nonnegativity of the vital functions or, in (H6), to reflect that the size of any individual in the population studied [23, 1, 24] is strictly increasing during its lifetime and never reaches the maximum value. Second, the mathematical requirements to obtain the existence and uniqueness of solutions to the problem (1.1)–(1.4), [21]. Last, the regularity properties needed in the numerical analysis to derive optimal rates of convergence [25].

The paper is structured as follows. In Section 2, we introduce the numerical methods we employ to make the integration of the problem (1.1)–(1.4). From Sections 3 to 6 we analyse the numerical schemes: first we introduce some preliminary results, then we prove the consistency and stability properties in order to obtain their convergence. In the final section we present numerical results which confirm the theoretical ones and the good behaviour of each numerical scheme when it approaches the stable steady state of a particular problem. The notation employed throughout the paper is given in Table 1.

2. Numerical integration

In this section, we describe the numerical methods employed for the integration of Eqs. (1.1)–(1.4). First, we rewrite the partial integro-differential equation in a more suitable form for its numerical treatment. Thus, we define

$$m(x, z, u, t) = \mu(x, z, t) + g_x(x, z, t) - g_z(x, z, t) \gamma(x) u.$$

Thus, (1.1) has the form

$$u_t(x, t) + g(x, B(x, t), t) u_x(x, t) = -m(x, B(x, t), u(x, t), t) u(x, t), \quad (2.6)$$

$x_m < x < x_M$, $t > 0$. Next, we denote by $x(t; t^*, x^*)$ the characteristic curve of Eq. (2.6) which takes the value x^* at time t^* . This is the solution to the following initial value problem,

$$\begin{cases} x'(t; t^*, x^*) = g(x(t; t^*, x^*), B(x(t; t^*, x^*), t), t), & t \geq t^*, \\ x(t^*; t^*, x^*) = x^*. \end{cases} \quad (2.7)$$

Note that $x(t; 0, x_M) = x_M$, $t \geq 0$; because we assume that $g(x_M, \cdot, \cdot) = 0$. Then, we define the function

$$w(t; t^*, x^*) = u(x(t; t^*, x^*), t), \quad t \geq t^*, \quad (2.8)$$

which satisfies the following initial value problem,

$$\begin{cases} \frac{d}{dt} w(t; t^*, x^*) = -m(x(t; t^*, x^*), B(x(t; t^*, x^*), t), w(t; t^*, x^*), t) w(t; t^*, x^*), & t \geq t^*, \\ w(t^*; t^*, x^*) = u(x^*, t^*), \end{cases} \quad (2.9)$$

and, therefore, it can be represented by the following formula

$$w(t; t^*, x^*) = u(x^*, t^*) \exp \left\{ - \int_{t^*}^t m(x(\tau; t^*, x^*), B(x(\tau; t^*, x^*), \tau), w(\tau; t^*, x^*), \tau) d\tau \right\}. \quad (2.10)$$

We suppose that $u(x_M, 0) = 0$ and then $u(x_M, t) = 0$, $t \geq 0$. We shall use this property in our numerical method. However, it can be easily modified to cover other cases.

Our numerical methods are based on the numerical integration along characteristics curves because these kind of schemes have shown its efficiency in other cases [25]. Also, other types of methods (like the total variation diminishing schemes) might not be suitable in simple situations in which the total variation of the solution **increases**. This situation could **happen** when the growth rate has no dependence on the population and $g_x + \mu < 0$ and, therefore, the solution could be unbounded. Also, when g_z is positive and the conditions of existence of Kraev [17] do not satisfy.

Now, we will introduce the numerical schemes we are going to use. The numerical integration along **with** characteristics means that the number of grid nodes increases **by** one at every time step because there is one node which fluxes from the minimum size, as we can see in [25]. Therefore, **first** we will introduce a numerical method which employs all the grid nodes obtained in the computation.

Let J and N be positive integers. We define the spatial and time discretization parameters as $h = \frac{x_M - x_m}{J}$ and $k = \frac{T}{N}$, respectively. We define the discrete time levels as $t_n = nk$, $0 \leq n \leq N$, and the initial grid nodes as $X_j^0 = x_m + jh$, $0 \leq j \leq J$. We suppose that the approximations to the theoretical solution at the initial time (ϕ in (1.3)) in such nodes are known, U_j^0 , $0 \leq j \leq J$. Thus, we denote

$$\mathbf{X}^0 = \{X_0^0 = x_m, X_1^0, \dots, X_{J-1}^0, X_J^0 = x_M\}, \quad \mathbf{U}^0 = \{U_0^0, U_1^0, \dots, U_{J-1}^0, U_J^0 = 0\},$$

the initial size grid and the initial approximation to the solution. Also, we introduce $\mathbf{I}^0 = \{I_0^0, I_1^0, \dots, I_{J-1}^0, I_J^0 = 0\}$, where

$$I_j^0 = Q_j(\mathbf{X}^0, \boldsymbol{\gamma}(\mathbf{X}^0) \mathbf{U}^0), \quad (2.11)$$

is defined as the discrete version of (1.4) at $x = X_j^0$, $j = 0, 1, \dots, J$, by using approximations to the integral term. In (2.11) and henceforth, the product of the vectors $\boldsymbol{\gamma}(\mathbf{X}) \mathbf{U}$ must be interpreted componentwise. In this case, we propose the following second-order composite quadrature rules throughout the paper; for $(p + 1)$ -dimensional vectors $\mathbf{X} = \{X_0, X_1, \dots, X_p\}$ and $\mathbf{V} = \{V_0, V_1, \dots, V_p\}$, representing the vector of nodes of the spatial grid and the vector of values of the function at the spatial grid, respectively,

$$Q_0(\mathbf{X}, \mathbf{V}) = V_1 (X_1 - x_m) + \sum_{l=1}^{p-1} \frac{X_{l+1} - X_l}{2} (V_l + V_{l+1}), \quad (2.12)$$

$$Q_j(\mathbf{X}, \mathbf{V}) = \sum_{l=j}^{p-1} \frac{X_{l+1} - X_l}{2} (V_l + V_{l+1}), \quad 1 \leq j \leq p - 1. \quad (2.13)$$

Expressions $\boldsymbol{\gamma}(\mathbf{X})$ and $\boldsymbol{\alpha}(\mathbf{X}, \mathbf{U})$ denote the vectors obtained from the evaluation of function $\boldsymbol{\gamma}$ and $\boldsymbol{\alpha}$ at the corresponding values.

We obtain the numerical approximations at time level t_1 as follows. First, we compute the following auxiliary values

$$X_0^{1,*} = x_m; \quad X_{j+1}^{1,*} = X_j^0 + k g(X_j^0, I_j^0, t_0), \quad 0 \leq j \leq J - 1; \quad X_{J+1}^{1,*} = x_M;$$

$$U_{j+1}^{1,*} = U_j^0 \exp(-k m(X_j^0, I_j^0, U_j^0, t_0)), \quad 0 \leq j \leq J - 1; \quad U_{J+1}^{1,*} = 0;$$

and $I_j^{1,*} = Q_j(\mathbf{X}^{1,*}, \boldsymbol{\gamma}(\mathbf{X}^{1,*}) \mathbf{U}^{1,*})$, $1 \leq j \leq J + 1$. These formulae are valid approximations for the solution to the problem, but they only contribute with **the** first convergence order and we want to build a second-order convergence scheme.

Then, we obtain the grid nodes $\mathbf{X}^1 = \{X_0^1 = x_m, X_1^1, \dots, X_{J+1}^1 = x_M\}$, by the numerical integration of (2.7) with the improved Euler method,

$$X_{j+1}^1 = X_j^0 + \frac{k}{2} \left(g(X_j^0, I_j^0, t_0) + g(X_{j+1}^{1,*}, I_{j+1}^{1,*}, t_1) \right), \quad (2.14)$$

$0 \leq j \leq J - 1$. Now, we calculate $\mathbf{U}^1 = \{U_0^1, U_1^1, \dots, U_J^1, U_{J+1}^1 = 0\}$, the corresponding approximations to the theoretical solution. For the approximation to the corresponding interior grid points, we use the following discretization of (2.10), based on the trapezoidal quadrature rule,

$$U_{j+1}^1 = U_j^0 \exp \left(-\frac{k}{2} \left(m(X_j^0, I_j^0, U_j^0, t_0) + m(X_{j+1}^{1,*}, I_{j+1}^{1,*}, U_{j+1}^{1,*}, t_1) \right) \right), \quad (2.15)$$

$0 \leq j \leq J - 1$. Then, we compute $I_j^1 = \mathcal{Q}_j(\mathbf{X}^1, \boldsymbol{\gamma}(\mathbf{X}^1) \mathbf{U}^1)$, $0 \leq j \leq J + 1$. Finally, we derive the approximation U_0^1 to $u(x_m, t_1)$ from a discrete version of the boundary condition (1.2)

$$U_0^1 = \frac{\Gamma(t_1) + \mathcal{Q}_0(\mathbf{X}^1, \boldsymbol{\alpha}(\mathbf{X}^1, \mathbf{U}^1) \mathbf{U}^1)}{g(x_m, I_0^1, t_1)}. \quad (2.16)$$

As in (2.11), we denote the componentwise product of the vectors $\boldsymbol{\alpha}(\mathbf{X}, \mathbf{U})$ and \mathbf{U} by $\boldsymbol{\alpha}(\mathbf{X}, \mathbf{U}) \mathbf{U}$. Note that the method introduces a new grid node which fluxes from the boundary. Thus, we set $J_0 = J$ and introduce the number of grid nodes at level t_1 as $J_1 + 1$, with $J_1 = J_0 + 1$. We also want to indicate that such a scheme is explicit.

Next, we describe the general time step t_{n+1} , $0 \leq n \leq N - 1$. Now, we suppose that the numerical approximations at the previous time level t_n are known,

$$\{X_0^n = x_m, X_1^n, \dots, X_{J_n-1}^n, X_{J_n}^n = x_M\}, \quad \{U_0^n, U_1^n, \dots, U_{J_n-1}^n, U_{J_n}^n = 0\},$$

and $\{I_0^n, I_1^n, \dots, I_{J_n-1}^n, I_{J_n}^n\}$, where J_n is the number of grid nodes at t_n . We recall that X_j^n and X_{j+1}^{n+1} , $0 \leq j \leq J_n - 1$, are (numerically) in the same characteristic curve. First, we compute the auxiliary values,

$$X_0^{n+1,*} = x_m; \quad X_{j+1}^{n+1,*} = X_j^n + k g(X_j^n, I_j^n, t_n), \quad 0 \leq j \leq J_n - 1;$$

$$U_{j+1}^{n+1,*} = U_j^n \exp(-k m(X_j^n, I_j^n, U_j^n, t_n)), \quad 0 \leq j \leq J_n - 1;$$

$$X_{J_n+1}^{n+1,*} = x_M; \quad U_{J_n+1}^{n+1,*} = 0;$$

and $I_j^{n+1,*} = \mathcal{Q}_j(\mathbf{X}^{n+1,*}, \boldsymbol{\gamma}(\mathbf{X}^{n+1,*}) \mathbf{U}^{n+1,*})$, $1 \leq j \leq J_n + 1$. We correct these values to obtain second-order approximations. The grid values at the time level t_{n+1} ,

$$\mathbf{X}^{n+1} = \{X_0^{n+1} = x_m, X_1^{n+1}, \dots, X_{J_n+1}^{n+1}, X_{J_n+1}^{n+1} = x_M\},$$

by means of the numerical integration of (2.7),

$$X_{j+1}^{n+1} = X_j^n + \frac{k}{2} \left(g(X_j^n, I_j^n, t_n) + g(X_{j+1}^{n+1,*}, I_{j+1}^{n+1,*}, t_{n+1}) \right), \quad (2.17)$$

$0 \leq j \leq J_n - 1$, and the approximations to the theoretical solution in these nodes at such a time level,

$$\mathbf{U}^{n+1} = \{U_0^{n+1}, U_1^{n+1}, \dots, U_{J_n}^{n+1}, U_{J_n+1}^{n+1} = 0\},$$

using the discretization of (2.10) for the approximation at the interior grid points,

$$U_{j+1}^{n+1} = U_j^n \exp \left(-\frac{k}{2} \left(m(X_j^n, I_j^n, U_j^n, t_n) + m(X_{j+1}^{n+1,*}, I_{j+1}^{n+1,*}, U_{j+1}^{n+1,*}, t_{n+1}) \right) \right), \quad (2.18)$$

$0 \leq j \leq J_n - 1$, and the approximation U_0^{n+1} to $u(x_m, t_{n+1})$, using a discretization of the boundary condition (1.2),

$$U_0^{n+1} = \frac{\Gamma(t_{n+1}) + \mathcal{Q}_0(\mathbf{X}^{n+1}, \boldsymbol{\alpha}(\mathbf{X}^{n+1}, \mathbf{U}^{n+1}) \mathbf{U}^{n+1})}{g(x_m, I_0^{n+1}, t_{n+1})}, \quad (2.19)$$

where $\boldsymbol{\alpha}_j(\mathbf{X}^{n+1}, \mathbf{U}^{n+1}) = \alpha(X_j^{n+1}, I_j^{n+1}, t_{n+1})$, $0 \leq j \leq J_n + 1$, and

$$I_j^{n+1} = \mathcal{Q}_j(\mathbf{X}^{n+1}, \boldsymbol{\gamma}(\mathbf{X}^{n+1}) \mathbf{U}^{n+1}), \quad 0 \leq j \leq J_n + 1.$$

We define $J_{n+1} = J_n + 1$. We observe that, at consecutive time levels, we work with a different number of nodes because we have introduced a new node which fluxes through the boundary. So, at time level t_n , we have $(J_n + 1)$ grid nodes and at time level t_{n+1} we have $(J_n + 2)$. This fact increases the memory requirements and computational cost. We could think of another kind of method which, at each time step, selects the nodes used in the numerical integration with different efficiency motivations. For example, we could propose a method which keeps the number of nodes constant at every time

step. Another possibility consists of selecting the grid nodes to obtain a suitable dynamic of the grid points in large time integration. These kind of schemes need a selection procedure after each time step.

Next, we describe the general setting when we introduce such a selection. The first time step integration is given by the Eqs. (2.14)–(2.16) and $J_1 = J + 1$. The equations of the general time integration t_{n+1} , $0 \leq n \leq N - 1$ are given by (2.17)–(2.19). At this moment, the treatment of the number of nodes in the subsequent levels of time has to be decided. As we pointed out, we could think of several strategies for the number of grid nodes. Therefore, we take the choice in the grid nodes which would continue the numerical integration and we consider J_{n+1} related to the number of grid nodes we set at time level t_{n+1} . For example, we could select some characteristic curves and we do not compute the approximations at such curves. We define λ_n as the first $l \in \mathbb{N}$ which satisfies

$$|X_{J_{n+1}}^{n+1} - X_{J_n - (l+1)}^{n+1}| > \beta h, \quad (2.20)$$

with β a fixed value. We eliminate the grid nodes $X_{J_n - l}^{n+1}$, $l = 0, \dots, \lambda_n - 1$. Also, we do not consider the corresponding values in the vectors \mathbf{U}^{n+1} and \mathbf{I}^{n+1} . Then, we define the value J_{n+1} as $J_n - \lambda_n + 1$, where $\lambda_n = 0$ means that we do not eliminate any node. Another possible choice involves eliminating the computation of the characteristic curve which begins at X_l^{n+1} , so that

$$|X_{J_{n+1}}^{n+1} - X_{l-1}^{n+1}| = \min_{1 \leq j \leq J_n} |X_{j+1}^{n+1} - X_{j-1}^{n+1}| \quad (2.21)$$

and the corresponding value in the vectors \mathbf{U}^{n+1} and \mathbf{I}^{n+1} . Then, we define the value J_{n+1} as J_n . Again, we should point out that the scheme is explicit.

3. Convergence analysis: preliminaries

In this section, we begin the analysis of a general class of numerical methods. More precisely, we consider a formulation in which, for each time level, all the nodes are considered, as were done in the method described by (2.14)–(2.19). However, at each time level, we have a quadrature rule which could be based on a subgrid. In this way, the numerical schemes with a selection procedure could be viewed as methods which employ quadrature rules based on the position of the nodes selected at each time step. When a node is eliminated, the quadrature rules considered for the following time steps do not take into account the position of this node as moving along the characteristic curve. Actually, the numerical methods as presented in the previous section do not compute the characteristic curves relative to those nodes to improve their efficiency, but to carry out our convergence analysis it is necessary to take into account all of them.

The convergence result will be obtained by means of consistency and nonlinear stability. In order to carry out this analysis, we have to rewrite it into the discretization framework developed by López-Marcos et al. [26].

We assume that the spatial discretization parameter, h , takes values in the set $H = \{h > 0 : h = (x_M - x_m)/J, J \in \mathbb{N}\}$. Now, we suppose that the time step, k , satisfies $k = r h$, where r is an arbitrary and positive constant fixed throughout the analysis. In addition, we set $N = \lceil T/k \rceil$. For each $h \in H$, we define the space

$$\mathcal{A}_h = \prod_{n=0}^N (\mathbb{R}^{J+n-1} \times \mathbb{R}^{J+n}),$$

where, for each time level n , $0 \leq n \leq N$, \mathbb{R}^{J+n-1} is used for the approximations to the interior grid nodes, and \mathbb{R}^{J+n} for those to the theoretical solution on them and on the left boundary node. We also consider the space

$$\mathcal{B}_h = (\mathbb{R}^{J-1} \times \mathbb{R}^J) \times \mathbb{R}^N \times \prod_{n=1}^N (\mathbb{R}^{J+n-1} \times \mathbb{R}^{J+n-1}),$$

where $(\mathbb{R}^{J-1} \times \mathbb{R}^J)$ is employed to compare with the initial approximations; \mathbb{R}^N considers the residuals which take place in the approximation to the solution at the boundary node for every time step; and $\prod_{n=1}^N (\mathbb{R}^{J+n-1} \times \mathbb{R}^{J+n-1})$, is used for the residuals which arise in the formulae which define the grid nodes and the solution values. We note that in spaces \mathcal{A}_h and \mathcal{B}_h , we do not consider the first and last grid nodes and the value of the solution at the last grid node because they are fixed values. Thus, both spaces have the same dimension.

In order to measure the size of the errors, we define

$$\|\boldsymbol{\eta}\|_\infty = \max_{1 \leq j \leq p} |\eta_j|, \quad \boldsymbol{\eta} = (\eta_1, \eta_2, \dots, \eta_p) \in \mathbb{R}^p,$$

$(B_\infty(\boldsymbol{\eta}, \rho)$ represents the corresponding open ball with centre $\boldsymbol{\eta}$ and radius $\rho > 0$), and

$$\|\mathbf{V}^n\|_1 = \sum_{j=0}^{J+n-1} h |V_j^n|, \quad \mathbf{V}^n \in \mathbb{R}^{J+n}.$$

Now, we endow spaces \mathcal{A}_h and \mathcal{B}_h with the following norms. If $(\mathbf{y}^0, \mathbf{v}^0, \dots, \mathbf{y}^N, \mathbf{v}^N) \in \mathcal{A}_h$, then

$$\|(\mathbf{y}^0, \mathbf{v}^0, \dots, \mathbf{y}^N, \mathbf{v}^N)\|_{\mathcal{A}_h} = \max\left(\max_{0 \leq n \leq N} \|\mathbf{y}^n\|_{\infty}, \max_{0 \leq n \leq N} \|\mathbf{v}^n\|_{\infty}\right).$$

On the other hand, if $(\mathbf{Y}^0, \mathbf{Z}^0, \mathbf{z}_0, \mathbf{Y}^1, \mathbf{Z}^1, \dots, \mathbf{Y}^N, \mathbf{Z}^N) \in \mathcal{B}_h$, then

$$\|(\mathbf{Y}^0, \mathbf{Z}^0, \mathbf{z}_0, \mathbf{Y}^1, \mathbf{Z}^1, \dots, \mathbf{Y}^N, \mathbf{Z}^N)\|_{\mathcal{B}_h} = \|\mathbf{Y}^0\|_{\infty} + \|\mathbf{Z}^0\|_{\infty} + \|\mathbf{z}_0\|_{\infty} + \sum_{n=1}^N k \|\mathbf{Z}^n\|_{\infty} + \sum_{n=1}^N k \|\mathbf{Y}^n\|_{\infty}.$$

For each $h \in H$, we define

$$\begin{aligned} \mathbf{x}_h &= (\mathbf{x}^0, \mathbf{x}^1, \mathbf{x}^2, \dots, \mathbf{x}^N), \\ \mathbf{x}^n &= (x_1^n, \dots, x_{j+n-1}^n) \in \mathbb{R}^{J+n-1}, \quad 0 \leq n \leq N, \\ x_j^0 &= x_m + jh, \quad 1 \leq j \leq J, \\ x_j^n &= x(t_n; t_{n-1}, x_{j-1}^{n-1}), \quad 1 \leq j \leq J+n-1, \quad 1 \leq n \leq N; \end{aligned} \quad (3.1)$$

and we denote $x_0^n = x_m$ and $x_{j+n}^n = x_M$, $n \geq 0$. Recall that $x(t; t^*, x^*)$ represents the theoretical solution to problem (1.5), $t^* \in [0, T]$, $x^* \in [x_m, x_M]$. In addition, if u represents the theoretical solution to (1.1)–(1.4) we define

$$\begin{aligned} \mathbf{u}_h &= (\mathbf{u}^0, \mathbf{u}^1, \mathbf{u}^2, \dots, \mathbf{u}^N), \\ \mathbf{u}^n &= (u_0^n, u_1^n, \dots, u_{j+n-1}^n) \in \mathbb{R}^{J+n}, \quad 0 \leq n \leq N, \\ u_j^n &= u(x_j^n, t_n), \quad 0 \leq j \leq J+n-1, \quad 0 \leq n \leq N, \end{aligned} \quad (3.2)$$

and we denote $u_{j+n}^n = 0$. Therefore, $\tilde{\mathbf{u}}_h = (\mathbf{x}^0, \mathbf{u}^0, \mathbf{x}^1, \mathbf{u}^1, \dots, \mathbf{x}^N, \mathbf{u}^N) \in \mathcal{A}_h$.

Next, we define the discretization operator. Let R be a positive constant and we denote by $B_{\mathcal{A}_h}(\tilde{\mathbf{u}}_h, Rh^p) \subset \mathcal{A}_h$ the open ball with centre $\tilde{\mathbf{u}}_h$ and radius Rh^p , $1 < p < 2$. Next, we introduce the operator

$$\begin{aligned} \Phi_h &: B_{\mathcal{A}_h}(\tilde{\mathbf{u}}_h, Rh^p) \rightarrow \mathcal{B}_h, \\ \Phi_h(\mathbf{y}^0, \mathbf{v}^0, \dots, \mathbf{y}^N, \mathbf{v}^N) &= (\mathbf{Y}^0, \mathbf{P}^0, \mathbf{P}_0, \mathbf{Y}^1, \mathbf{P}^1, \dots, \mathbf{Y}^N, \mathbf{P}^N), \end{aligned} \quad (3.3)$$

defined by the following equations,

$$\mathbf{Y}^0 = \mathbf{y}^0 - \mathbf{X}^0 \in \mathbb{R}^J, \quad (3.4)$$

$$\mathbf{P}^0 = \mathbf{v}^0 - \mathbf{U}^0 \in \mathbb{R}^{J+1}. \quad (3.5)$$

Vectors \mathbf{X}^0 and \mathbf{U}^0 represent approximations at $t = 0$, respectively, to the initial grid nodes and to the theoretical solution at them. Also,

$$P_0^{n+1} = V_0^{n+1} - \frac{\Gamma(t_{n+1}) + \mathcal{Q}_0^{n+1}(\mathbf{y}^{n+1}, \boldsymbol{\alpha}(\mathbf{y}^{n+1}, \mathbf{v}^{n+1}) \mathbf{v}^{n+1})}{g(x_m, \mathcal{Q}_0^{n+1}(\mathbf{y}^{n+1}, \boldsymbol{\gamma}(\mathbf{y}^{n+1}) \mathbf{v}^{n+1}), t_{n+1})}, \quad (3.6)$$

$$\begin{aligned} Y_{j+1}^{n+1} &= \frac{1}{k} \left\{ y_{j+1}^{n+1} - y_j^n - \frac{k}{2} \left(g(y_j^n, \mathcal{Q}_j^n(\mathbf{y}^n, \boldsymbol{\gamma}(\mathbf{y}^n) \mathbf{v}^n), t_n) \right. \right. \\ &\quad \left. \left. + g(y_{j+1}^{n+1,*}, \mathcal{Q}_{j+1}^{n+1}(\mathbf{y}^{n+1,*}, \boldsymbol{\gamma}(\mathbf{y}^{n+1,*}) \mathbf{v}^{n+1,*}), t_{n+1}) \right) \right\}, \end{aligned} \quad (3.7)$$

$$\begin{aligned} P_{j+1}^{n+1} &= \frac{1}{k} \left\{ V_{j+1}^{n+1} - V_j^n \exp\left(-\frac{k}{2} \left(m(y_j^n, \mathcal{Q}_j^n(\mathbf{y}^n, \boldsymbol{\gamma}(\mathbf{y}^n) \mathbf{v}^n), V_j^n, t_n) \right. \right. \right. \\ &\quad \left. \left. + m(y_{j+1}^{n+1,*}, \mathcal{Q}_{j+1}^{n+1}(\mathbf{y}^{n+1,*}, \boldsymbol{\gamma}(\mathbf{y}^{n+1,*}) \mathbf{v}^{n+1,*}), V_{j+1}^{n+1,*}, t_{n+1}) \right) \right\}, \end{aligned} \quad (3.8)$$

$0 \leq j \leq J+n-1$, $0 \leq n \leq N-1$. Where, with the notation introduced in Section 2,

$$\begin{aligned} y_0^{n+1,*} &= x_m, \quad y_{j+n+1}^{n+1,*} = x_M, \\ y_{j+1}^{n+1,*} &= y_j^n + kg(y_j^n, \mathcal{Q}_j^n(\mathbf{y}^n, \boldsymbol{\gamma}(\mathbf{y}^n) \mathbf{v}^n), t_n), \quad 0 \leq j \leq J+n-1, \end{aligned} \quad (3.9)$$

$$\begin{aligned} V_{j+1}^{n+1,*} &= V_j^n \exp(-km(y_j^n, \mathcal{Q}_j^n(\mathbf{y}^n, \boldsymbol{\gamma}(\mathbf{y}^n) \mathbf{v}^n), V_j^n, t_n)), \quad 0 \leq j \leq J+n-1, \\ V_{j+n+1}^{n+1,*} &= 0, \end{aligned} \quad (3.10)$$

$0 \leq n \leq N-1$, $\alpha_j^n(\mathbf{y}, \mathbf{V}) = \alpha(y_j^n, \mathcal{Q}_j^n(\mathbf{y}, \boldsymbol{\gamma}(\mathbf{y}) \mathbf{V}), t_n)$, $\gamma_j^n(\mathbf{y}) = \gamma(y_j^n)$, $0 \leq j \leq J+n$, $1 \leq n \leq N$; $\gamma_j^{n,*}(\mathbf{y}) = \gamma(y_j^{n,*})$, $0 \leq j \leq J+n+1$. On the other hand, we denote by

$$\mathcal{Q}_0^n(\mathbf{X}, \mathbf{V}) = \sum_{l=1}^{J+n} q_l^{n,0}(\mathbf{X}) V_l, \quad \mathcal{Q}_j^n(\mathbf{X}, \mathbf{V}) = \sum_{l=j}^{J+n} q_l^{n,j}(\mathbf{X}) V_l,$$

the general quadrature rules employed at each time level. These quadrature rules use fixed values for nodes $y_0^n = x_0^n = x_m$, $y_{J+n}^n = x_{J+n}^n = x_M$, and for the solution $V_{J+n}^n = V_{J+n}^n = 0$, $0 \leq n \leq N$.

Note that, Φ_h takes into account all the possible nodes and their corresponding solution values at each time level, and it employs quadrature rules possibly based on a subgrid. If $\tilde{\mathbf{U}}_h = (\mathbf{X}^0, \mathbf{U}^0, \mathbf{X}^1, \mathbf{U}^1, \dots, \mathbf{X}^N, \mathbf{U}^N) \in B_{\mathcal{A}_h}(\tilde{\mathbf{u}}_h, R h^p)$, satisfies

$$\Phi_h(\tilde{\mathbf{U}}_h) = \mathbf{0} \in \mathcal{B}_h, \quad (3.11)$$

the nodes and the corresponding values to the solution at such nodes of $\tilde{\mathbf{U}}_h$ are a numerical solution to the scheme defined by (2.14)–(2.19) when the quadrature rules are given by (2.12)–(2.13). On the other hand, the numerical solution to the scheme defined by (2.14)–(2.19) satisfies (3.11).

Henceforth, C will denote a positive constant, independent of h , k ($k = r h$), j ($0 \leq j \leq J+n$) and n ($0 \leq n \leq N$); C possibly has different values in different places. Now, we introduce the following properties that we suppose the quadrature rules satisfy. These are the sufficient properties the quadrature rules have to satisfy to carry out our convergence analysis.

(P1) $|B(x_j^n, t_n) - \mathcal{Q}_j^n(\mathbf{x}^n, \boldsymbol{\gamma}(\mathbf{x}^n) \mathbf{u}^n)| \leq C h^2$, if $h \rightarrow 0$, where $\gamma_j(\mathbf{x}^n) = \gamma(x_j^n)$, $0 \leq j \leq J+n$, $0 \leq n \leq N$.

(P2) $\left| \int_{x_m}^{x_M} \alpha(x, B(x, t_n), t_n) u(x, t_n) dx - \mathcal{Q}_0^n(\mathbf{x}^n, \alpha(\mathbf{x}^n, \mathbf{B}^n) \mathbf{u}^n) \right| \leq C h^2$, if $h \rightarrow 0$, $0 \leq n \leq N$. Where $\alpha_j^n(\mathbf{x}^n, \mathbf{B}^n) = \alpha(x_j^n, B(x_j^n, t_n), t_n)$, $0 \leq j \leq J+n$, $0 \leq n \leq N$.

(P3) $|q_i^{n,j}(\mathbf{x}^n)| \leq q h$, where q is a positive constant independent of h , k ($k = r h$), j ($0 \leq j \leq J+n$) and n ($0 \leq n \leq N$), $j \leq i \leq J+n$, $0 \leq j \leq J+n$, $0 \leq n \leq N$.

(P4) Let R and p be positive constants with $1 < p < 2$. The functions $q_i^{n,j}$ are Lipschitz continuous in $B_\infty(\mathbf{x}^n, R h^p)$, $j \leq i \leq J+n$, $0 \leq j \leq J+n$, $0 \leq n \leq N$.

(P5) Let R and p be positive constants with $1 < p < 2$. If $\mathbf{y}^n, \mathbf{z}^n \in B_\infty(\mathbf{x}^n, R h^p)$ and $\mathbf{V}^n \in B_\infty(\mathbf{u}^n, R h^p)$,

$$|\mathcal{Q}_j^n(\mathbf{y}^n, \boldsymbol{\gamma}(\mathbf{z}^n) \mathbf{V}^n) - \mathcal{Q}_j^n(\mathbf{z}^n, \boldsymbol{\gamma}(\mathbf{z}^n) \mathbf{V}^n)| \leq C \|\mathbf{y}^n - \mathbf{z}^n\|_\infty,$$

if $h \rightarrow 0$, $0 \leq j \leq J+n$, $0 \leq n \leq N$.

(P6) Let R and p be positive constants with $1 < p < 2$. If $\mathbf{y}^n, \mathbf{z}^n \in B_\infty(\mathbf{x}^n, R h^p)$ and $\mathbf{V}^n \in B_\infty(\mathbf{u}^n, R h^p)$,

$$|\mathcal{Q}_j^n(\mathbf{y}^n, \alpha(\mathbf{z}^n, \mathbf{V}^n) \mathbf{V}^n) - \mathcal{Q}_j^n(\mathbf{z}^n, \alpha(\mathbf{z}^n, \mathbf{V}^n) \mathbf{V}^n)| \leq C \|\mathbf{y}^n - \mathbf{z}^n\|_\infty,$$

if $h \rightarrow 0$, $0 \leq j \leq J+n$, $0 \leq n \leq N$.

The following result shows that operator (3.3) is well defined.

Proposition 1. Let us assume that hypotheses (H1)–(H6) about problem (1.1)–(1.4), and properties (P1)–(P6) of the quadrature rules hold. If

$$(\mathbf{X}^0, \mathbf{V}^0, \dots, \mathbf{X}^N, \mathbf{V}^N) \in B_{\mathcal{A}_h}(\tilde{\mathbf{u}}_h, R h^p),$$

where R is a fixed positive constant and $1 < p < 2$, then, for h sufficiently small,

$$\mathcal{Q}_j^n(\mathbf{X}^n, \boldsymbol{\gamma}(\mathbf{X}^n) \mathbf{V}^n) \in D_B, \quad (3.12)$$

$0 \leq n \leq N$, and

$$\mathcal{Q}_j^n(\mathbf{X}^{n,*}, \boldsymbol{\gamma}(\mathbf{X}^{n,*}) \mathbf{V}^{n,*}) \in D_B, \quad (3.13)$$

$0 \leq n \leq N-1$.

Proof. The definition of \mathcal{Q}_j^n , the hypotheses (H1)–(H6), the properties (P1)–(P6) and that \mathbf{V}^n is bounded, allow us to obtain

$$\begin{aligned} & |\mathcal{Q}_j^n(\mathbf{X}^n, \boldsymbol{\gamma}(\mathbf{X}^n) \mathbf{V}^n) - B(x_j^n, t_n)| \leq C \|\mathbf{X}^n - \mathbf{x}^n\|_\infty \\ & + \left| \sum_{l=j}^{J+n} q_l^{n,j}(\mathbf{X}) (\gamma(X_l^n) - \gamma(x_l^n)) V_l \right| + \left| \sum_{l=j}^{J+n} q_l^{n,j}(\mathbf{X}) \gamma(x_l^n) (V_l - u_l^n) \right| + o(1) \\ & \leq C R h^p + C q R h^{p+1} (J+n-j+1) (\|\mathbf{V}^n\|_\infty + \|\gamma\|_\infty) + o(1), \end{aligned} \quad (3.14)$$

$0 \leq j \leq J+n$, $0 \leq n \leq N$, $h \rightarrow 0$. Therefore, (3.12) holds for h sufficiently small. On the other hand, (3.13) is easily derived following the same arguments. \square

On the other hand, the quadrature rules employed in the numerical methods presented in Section 2 could be written into this notation as

$$\mathcal{Q}_0^n(\mathbf{X}, \mathbf{V}) = V_{\lambda_1^n} (X_{\lambda_1^n} - x_m) + \sum_{l=1}^{J_n-1} \frac{X_{\lambda_{l+1}^n} - X_{\lambda_l^n}}{2} (V_{\lambda_l^n} + V_{\lambda_{l+1}^n}), \quad (3.15)$$

$$\mathcal{Q}_j^n(\mathbf{X}, \mathbf{V}) = V_{\lambda_{l(j)}^n} (X_{\lambda_{l(j)}^n} - X_j) + \sum_{l=l(j)}^{J_n-1} \frac{X_{\lambda_{l+1}^n} - X_{\lambda_l^n}}{2} (V_{\lambda_l^n} + V_{\lambda_{l+1}^n}), \quad (3.16)$$

$1 \leq j \leq J + n - 1$, where $\lambda_{l(j)}^n$ corresponds to the first subindex in the subgrid with $j \leq \lambda_{l(j)}^n$. If we consider this choice of quadrature rules, it is shown that they satisfy the properties (P1)–(P6).

Theorem 1. Let us assume that the hypotheses (H1)–(H6) about problem (1.1)–(1.4) hold. Let R and p be positive constants with

$1 < p < 2$. If $\mathbf{y}^n, \mathbf{z}^n \in B_\infty(\mathbf{x}^n, R h^p)$ and $\mathbf{V}^n \in B_\infty(\mathbf{u}^n, R h^p)$ and $\{x_{\lambda_l^n}^n\}_{l=0}^{J_n}$, $0 \leq n \leq N$, are subgrids with the property

(SG) There exists a positive constant C such that, for h sufficiently small, $x_{\lambda_{l+1}^n}^n - x_{\lambda_l^n}^n \leq C h$, $0 \leq l \leq J_n - 1$, $x_{\lambda_0^n}^n = x_m$, $x_{\lambda_{J_n}^n}^n = x_{j+n}^n$,

with $\{x_{\lambda_l^n}^n\}_{l=0}^{J_n}$ contained in \mathbf{x}^n , $0 \leq n \leq N$.

Thus, the quadrature rules (3.15)–(3.16) satisfy properties (P1)–(P6).

Proof. We note that properties (P1)–(P4) can be easily derived under our assumptions by means of property (SG) and the properties of the composite trapezoidal quadrature rule and the rectangular quadrature rule. On the other hand, proof of (P5) and (P6) is very similar. Therefore, we will establish (P5) and omit the proof of (P6).

We will rewrite the formula in this way

$$\begin{aligned} \mathcal{Q}_j^n(\mathbf{y}^n, \boldsymbol{\gamma}(\mathbf{z}^n) \mathbf{V}^n) - \mathcal{Q}_j^n(\mathbf{z}^n, \boldsymbol{\gamma}(\mathbf{z}^n) \mathbf{V}^n) &= \left((y_{\lambda_{l(j)}^n}^n - z_{\lambda_{l(j)}^n}^n) - (y_j^n - z_j^n) \right) \gamma(z_{\lambda_{l(j)}^n}^n) V_{\lambda_{l(j)}^n}^n \\ &- \sum_{l=l(j)+1}^{J_n-1} \frac{y_{\lambda_l^n}^n - z_{\lambda_l^n}^n}{2} \left(\gamma(z_{\lambda_{l+1}^n}^n) V_{\lambda_{l+1}^n}^n - \gamma(z_{\lambda_{l-1}^n}^n) V_{\lambda_{l-1}^n}^n \right) - \frac{y_{\lambda_{l(j)}^n}^n - z_{\lambda_{l(j)}^n}^n}{2} \left(\gamma(z_{\lambda_{l(j)+1}^n}^n) V_{\lambda_{l(j)+1}^n}^n + \gamma(z_{\lambda_{l(j)}^n}^n) V_{\lambda_{l(j)}^n}^n \right) \\ &+ \frac{y_{\lambda_{j_n}^n}^n - z_{\lambda_{j_n}^n}^n}{2} \left(\gamma(z_{\lambda_{j-1}^n}^n) V_{\lambda_{j-1}^n}^n + \gamma(z_{\lambda_j^n}^n) V_{\lambda_j^n}^n \right). \end{aligned} \quad (3.17)$$

Now, the hypotheses (H1)–(H6), $\|\mathbf{V}^n\|_\infty < \infty$, and the property (SG), allow us to obtain

$$\begin{aligned} \left| \gamma(z_{\lambda_{l+1}^n}^n) V_{\lambda_{l+1}^n}^n - \gamma(z_{\lambda_{l-1}^n}^n) V_{\lambda_{l-1}^n}^n \right| &\leq \left| \left(\gamma(z_{\lambda_{l+1}^n}^n) - \gamma(x_{\lambda_{l+1}^n}^n) \right) V_{\lambda_{l+1}^n}^n \right| \\ &+ \left| \left(\gamma(z_{\lambda_{l-1}^n}^n) - \gamma(x_{\lambda_{l-1}^n}^n) \right) V_{\lambda_{l-1}^n}^n \right| + \left| \gamma(x_{\lambda_{l+1}^n}^n) (V_{\lambda_{l+1}^n}^n - u_{\lambda_{l+1}^n}^n) \right| \\ &+ \left| \gamma(x_{\lambda_{l-1}^n}^n) (V_{\lambda_{l-1}^n}^n - u_{\lambda_{l-1}^n}^n) \right| + \left| \gamma(x_{\lambda_{l+1}^n}^n) u_{\lambda_{l+1}^n}^n - \gamma(x_{\lambda_{l-1}^n}^n) u_{\lambda_{l-1}^n}^n \right| \\ &\leq C(h^p + h), \end{aligned} \quad (3.18)$$

$l(j) + 1 \leq l \leq J_n - 1$. Thus, by means of (3.17)–(3.18) and $J_n \leq (C_1 h)^{-1}$, we obtain

$$\begin{aligned} |\mathcal{Q}_j^n(\mathbf{y}^n, \boldsymbol{\gamma}(\mathbf{z}^n) \mathbf{V}^n) - \mathcal{Q}_j^n(\mathbf{z}^n, \boldsymbol{\gamma}(\mathbf{z}^n) \mathbf{V}^n)| &\leq C \|\mathbf{y}^n - \mathbf{z}^n\|_\infty (1 + (h^p + h) (J_n - 1 - l(j))) \\ &\leq C \|\mathbf{y}^n - \mathbf{z}^n\|_\infty \end{aligned} \quad (3.19)$$

as desired. \square

4. Consistency

We define the local discretization error as

$$\mathbf{I}_h = \Phi_h(\tilde{\mathbf{u}}_h) \in \mathcal{B}_h,$$

and we say that the discretization (3.3) is consistent if, as $h \rightarrow 0$,

$$\lim \|\Phi_h(\tilde{\mathbf{u}}_h)\|_{\mathcal{B}_h} = \lim \|\mathbf{I}_h\|_{\mathcal{B}_h} = 0.$$

The following theorem establishes the consistency of the numerical scheme defined by Eqs. (3.4)–(3.8).

Theorem 2. Let us assume that hypotheses (H1)–(H6) about problem (1.1)–(1.4), and properties (P1)–(P6) of the quadrature rule hold. Then, as $h \rightarrow 0$, the local discretization error satisfies,

$$\|\Phi_h(\tilde{\mathbf{u}}_h)\|_{\mathcal{B}_h} = \|\mathbf{u}^0 - \mathbf{U}^0\|_\infty + \|\mathbf{x}^0 - \mathbf{X}^0\|_\infty + O(h^2 + k^2). \quad (4.1)$$

Proof. We denote $\Phi_h(\tilde{\mathbf{u}}_h) = (\mathbf{Z}^0, \mathbf{L}^0, \mathbf{L}_0, \mathbf{Z}^1, \mathbf{L}^1, \dots, \mathbf{Z}^N, \mathbf{L}^N)$.

First, we set bounds for the auxiliary values. Then, by means of the definitions (3.9)–(3.10), the regularity hypotheses (H1)–(H6), the property (P1) and the error bound for the explicit Euler method and the rectangular quadrature rule, we obtain

$$\begin{aligned} |x_j^n - x_j^{n,*}| &\leq |x(t_n; t_{n-1}, x_{j-1}^{n-1}) - x_{j-1}^{n-1} - k g(x_{j-1}^{n-1}, B(x_{j-1}^{n-1}, t_{n-1}), t_{n-1})| \\ &\quad + k |g(x_{j-1}^{n-1}, B(x_{j-1}^{n-1}, t_{n-1}), t_{n-1}) - g(x_{j-1}^{n-1}, \mathcal{Q}_{j-1}^{n-1}(\mathbf{x}^{n-1}, \boldsymbol{\gamma}(\mathbf{x}^{n-1}) \mathbf{u}^{n-1}), t_{n-1})| \\ &\leq C k^2 + C k |B(x_{j-1}^{n-1}, t_{n-1}) - \mathcal{Q}_{j-1}^{n-1}(\mathbf{x}^{n-1}, \boldsymbol{\gamma}(\mathbf{x}^{n-1}) \mathbf{u}^{n-1})| \\ &\leq C (k^2 + h^2), \end{aligned} \quad (4.2)$$

$1 \leq j \leq J + n - 1$, and

$$\begin{aligned} |u_j^n - u_j^{n,*}| &\leq C \left| \int_{t_{n-1}}^{t_n} m(x(\tau; t_{n-1}, x_{j-1}^{n-1}), B(x(\tau; t_{n-1}, x_{j-1}^{n-1}), \tau), u(x(\tau; t_{n-1}, x_{j-1}^{n-1}), \tau), \tau) d\tau \right. \\ &\quad \left. - k m(x_{j-1}^{n-1}, B(x_{j-1}^{n-1}, t_{n-1}), u_{j-1}^{n-1}, t_{n-1}) \right| + C k |m(x_{j-1}^{n-1}, B(x_{j-1}^{n-1}, t_{n-1}), u_{j-1}^{n-1}, t_{n-1}) \\ &\quad - m(x_{j-1}^{n-1}, \mathcal{Q}_{j-1}^{n-1}(\mathbf{x}^{n-1}, \boldsymbol{\gamma}(\mathbf{x}^{n-1}) \mathbf{u}^{n-1}), u_{j-1}^{n-1}, t_{n-1})| \\ &\leq C k^2 + C k |B(x_{j-1}^{n-1}, t_{n-1}) - \mathcal{Q}_{j-1}^{n-1}(\mathbf{x}^{n-1}, \boldsymbol{\gamma}(\mathbf{x}^{n-1}) \mathbf{u}^{n-1})| \\ &\leq C (k^2 + h^2), \end{aligned} \quad (4.3)$$

$1 \leq j \leq J + n - 1$, $1 \leq n \leq N$.

Now, we set the bounds for \mathbf{Z}^n , $1 \leq n \leq N$. By means of (2.7) and (3.7), the regularity hypotheses (H1)–(H6), the property (P1), inequalities (4.2)–(4.3), and the error bound of R-K schemes employed, we have

$$\begin{aligned} |Z_j^n| &= \frac{1}{k} \left| x_j^n - x_{j-1}^{n-1} - \frac{k}{2} \{g(x_{j-1}^{n-1}, \mathcal{Q}_{j-1}^{n-1}(\mathbf{x}^{n-1}, \boldsymbol{\gamma}(\mathbf{x}^{n-1}) \mathbf{u}^{n-1}), t_{n-1}) + g(x_j^{n,*}, \mathcal{Q}_j^n(\mathbf{x}^{n,*}, \boldsymbol{\gamma}(\mathbf{x}^{n,*}) \mathbf{u}^{n,*}), t_n)\} \right| \\ &\leq C \{k^2 + |B(x_{j-1}^{n-1}, t_{n-1}) - \mathcal{Q}_{j-1}^{n-1}(\mathbf{x}^{n-1}, \boldsymbol{\gamma}(\mathbf{x}^{n-1}) \mathbf{u}^{n-1})|\} + C \{|x_j^n - x_j^{n,*}| + |B(x_j^n, t_n) - B(x_j^{n,*}, t_n)|\} \\ &\quad + C |B(x_j^{n,*}, t_n) - \mathcal{Q}_j^n(\mathbf{x}^{n,*}, \boldsymbol{\gamma}(\mathbf{x}^{n,*}) \mathbf{u}^{n,*})| \\ &\quad + C |\mathcal{Q}_j^n(\mathbf{x}^{n,*}, \boldsymbol{\gamma}(\mathbf{x}^{n,*}) \mathbf{u}^{n,*}) - \mathcal{Q}_j^n(\mathbf{x}^{n,*}, \boldsymbol{\gamma}(\mathbf{x}^{n,*}) \mathbf{u}^{n,*})| \\ &\leq C (k^2 + h^2), \end{aligned} \quad (4.4)$$

$1 \leq j \leq J + n - 1$, $1 \leq n \leq N$. Next, analogous arguments to those used to derive (4.4) lead us to establish the bound for the truncation errors produced by the solution to the PDE. By means of (2.10) and (3.8), the regularity hypotheses (H1)–(H6), the property (P1) of the quadrature rule, inequalities (4.2)–(4.3), and the error bound of the trapezoidal quadrature rule, we have

$$\begin{aligned} |L_j^n| &\leq \frac{1}{k} |u_{j-1}^{n-1}| \left| \exp \left\{ - \int_{t_{n-1}}^{t_n} m(x(\tau; t_{n-1}, x_{j-1}^{n-1}), B(x(\tau; t_{n-1}, x_{j-1}^{n-1}), \tau), u(x(\tau; t_{n-1}, x_{j-1}^{n-1}), \tau), \tau) d\tau \right\} \right. \\ &\quad \left. - \exp \left\{ - \frac{k}{2} (m(x_{j-1}^{n-1}, \mathcal{Q}_{j-1}^{n-1}(\mathbf{x}^{n-1}, \boldsymbol{\gamma}(\mathbf{x}^{n-1}) \mathbf{u}^{n-1}), u_{j-1}^{n-1}, t_{n-1}) \right. \right. \\ &\quad \left. \left. + m(x_j^{n,*}, \mathcal{Q}_j^n(\mathbf{x}^{n,*}, \boldsymbol{\gamma}(\mathbf{x}^{n,*}) \mathbf{u}^{n,*}), u_j^{n,*}, t_n)) \right\} \right| \\ &\leq C k^2 + C |B(x_{j-1}^{n-1}, t_{n-1}) - \mathcal{Q}_{j-1}^{n-1}(\mathbf{x}^{n-1}, \boldsymbol{\gamma}(\mathbf{x}^{n-1}) \mathbf{u}^{n-1})| \\ &\quad + C |x_j^n - x_j^{n,*}| + C |B(x_j^n, t_n) - B(x_j^{n,*}, t_n)| + C |u_j^n - u_j^{n,*}| \\ &\quad + C |B(x_j^{n,*}, t_n) - \mathcal{Q}_j^n(\mathbf{x}^{n,*}, \boldsymbol{\gamma}(\mathbf{x}^{n,*}) \mathbf{u}^{n,*})| \\ &\quad + C |\mathcal{Q}_j^n(\mathbf{x}^{n,*}, \boldsymbol{\gamma}(\mathbf{x}^{n,*}) \mathbf{u}^{n,*}) - \mathcal{Q}_j^n(\mathbf{x}^{n,*}, \boldsymbol{\gamma}(\mathbf{x}^{n,*}) \mathbf{u}^{n,*})| \\ &\leq C (k^2 + h^2), \end{aligned} \quad (4.5)$$

$1 \leq j \leq J + n - 1$, $1 \leq n \leq N$.

Finally, in order to find an estimate for the boundary terms, the hypotheses (H1)–(H6) and the properties (P1)–(P2) allow us to obtain

$$\begin{aligned} & \left| \int_{x_m}^{x_M} \alpha(x, B(x, t_n), t_n) u(x, t_n) dx - \mathcal{Q}_0^n(\mathbf{x}^n, \boldsymbol{\alpha}(\mathbf{x}^n, \mathbf{u}^n) \mathbf{u}^n) \right| \\ & \leq \left| \int_{x_m}^{x_M} \alpha(x, B(x, t_n)) u(x, t_n) dx - \mathcal{Q}_0^n(\mathbf{x}^n, \boldsymbol{\alpha}(\mathbf{x}^n, \mathbf{B}^n) \mathbf{u}^n) \right| + \left| \mathcal{Q}_0^n(\mathbf{x}^n, \boldsymbol{\alpha}(\mathbf{x}^n, \mathbf{B}^n) \mathbf{u}^n) - \mathcal{Q}_0^n(\mathbf{x}^n, \boldsymbol{\alpha}(\mathbf{x}^n, \mathbf{u}^n) \mathbf{u}^n) \right| \\ & \leq C h^2, \end{aligned} \quad (4.6)$$

$1 \leq n \leq N$. Then, by means of (3.6), hypothesis (H6), property (P1) and inequality (4.6), we have

$$\begin{aligned} |L_0^n| & \leq C \left\{ \left| g(x_m, B(x_m, t_n), t_n) - g(x_m, \mathcal{Q}_0^n(\mathbf{x}^n, \boldsymbol{\gamma}(\mathbf{x}^n) \mathbf{u}^n), t_n) \right| |u_0^n| \right. \\ & \quad \left. + \left| \int_{x_m}^{x_M} \alpha(x, B(x, t_n), t_n) u(x, t_n) dx - \mathcal{Q}_0^n(\mathbf{x}^n, \boldsymbol{\alpha}(\mathbf{x}^n, \mathbf{u}^n) \mathbf{u}^n) \right| \right\} \\ & \leq C \{ |B(x_m, t_n) - \mathcal{Q}_0^n(\mathbf{x}^n, \boldsymbol{\gamma}(\mathbf{x}^n) \mathbf{u}^n)| + h^2 \} \\ & \leq C h^2, \end{aligned} \quad (4.7)$$

$1 \leq n \leq N$.

Therefore, (4.1) follows from (4.4)–(4.5) and (4.7). \square

5. Stability

Another notion which plays an important role in the analysis of the numerical method is the *stability with h-dependent thresholds*. For $h \in H$, let R_h be a real number (*the stability threshold*) with $0 < R_h < \infty$: we say that the discretization (3.3) is *stable for $\tilde{\mathbf{u}}_h$* restricted to the thresholds R_h , if there exist two positive constants h_0 and S (*the stability constant*) such that, for any $h \in H$ with $h \leq h_0$, the open ball $B_{\mathcal{A}_h}(\tilde{\mathbf{u}}_h, R_h)$ is contained in the domain of Φ_h and for all $\tilde{\mathbf{V}}_h, \tilde{\mathbf{W}}_h$ in that ball,

$$\|\tilde{\mathbf{V}}_h - \tilde{\mathbf{W}}_h\|_{\mathcal{A}_h} \leq S \|\Phi_h(\tilde{\mathbf{V}}_h) - \Phi_h(\tilde{\mathbf{W}}_h)\|_{\mathcal{B}_h}.$$

We begin with the following auxiliary results.

Proposition 2. Let us assume that hypotheses (H1)–(H6) about problem (1.1)–(1.4), and properties (P1)–(P6) of the quadrature rule hold. Let $\mathbf{y}^n, \mathbf{z}^n \in B_\infty(\mathbf{x}^n, R h^p)$ and $\mathbf{V}^n, \mathbf{W}^n \in B_\infty(\mathbf{u}^n, R h^p)$. Then, as $h \rightarrow 0$,

$$|\mathcal{Q}_j^n(\mathbf{y}, \boldsymbol{\gamma}(\mathbf{y}) \mathbf{V}) - \mathcal{Q}_j^n(\mathbf{z}, \boldsymbol{\gamma}(\mathbf{z}) \mathbf{W})| \leq C (\|\mathbf{V}^n - \mathbf{W}^n\|_1 + \|\mathbf{y}^n - \mathbf{z}^n\|_\infty), \quad (5.1)$$

$0 \leq j \leq J + n, 1 \leq n \leq N$.

Proof. The triangle inequality, hypotheses (H2), properties (P3), (P5) and that $\|\mathbf{W}^n\|_\infty \leq C$ yield

$$\begin{aligned} |\mathcal{Q}_j^n(\mathbf{y}, \boldsymbol{\gamma}(\mathbf{y}) \mathbf{V}) - \mathcal{Q}_j^n(\mathbf{z}, \boldsymbol{\gamma}(\mathbf{z}) \mathbf{W})| & \leq C \sum_{l=j}^{J+n} h |V_l^n - W_l^n| + C \sum_{l=j}^{J+n} h |y_l^n - z_l^n| + \|\mathbf{y}^n - \mathbf{z}^n\|_\infty \\ & \leq C (\|\mathbf{V}^n - \mathbf{W}^n\|_1 + \|\mathbf{y}^n - \mathbf{z}^n\|_\infty), \end{aligned}$$

$1 \leq n \leq N$, as desired. \square

Proposition 3. Let us assume that hypotheses (H1)–(H6) about problem (1.1)–(1.4), and properties (P1)–(P6) of the quadrature rule hold. Let $\mathbf{y}^n, \mathbf{z}^n \in B_\infty(\mathbf{x}^n, R h^p)$ and $\mathbf{V}^n, \mathbf{W}^n \in B_\infty(\mathbf{u}^n, R h^p)$. Then, as $h \rightarrow 0$,

$$|y_j^{n,*} - z_j^{n,*}| \leq (1 + C k) |y_{j-1}^{n-1} - z_{j-1}^{n-1}| + C k \|\mathbf{y}^{n-1} - \mathbf{z}^{n-1}\|_\infty + C k \|\mathbf{V}^{n-1} - \mathbf{W}^{n-1}\|_1, \quad (5.2)$$

$$|V_j^{n,*} - W_j^{n,*}| \leq (1 + C k) |V_{j-1}^{n-1} - W_{j-1}^{n-1}| + C k \|\mathbf{y}^{n-1} - \mathbf{z}^{n-1}\|_\infty + C k \|\mathbf{V}^{n-1} - \mathbf{W}^{n-1}\|_1, \quad (5.3)$$

$$|\mathcal{Q}_j^n(\mathbf{y}^{n,*}, \boldsymbol{\gamma}(\mathbf{y}^{n,*}) \mathbf{V}^{n,*}) - \mathcal{Q}_j^n(\mathbf{z}^{n,*}, \boldsymbol{\gamma}(\mathbf{z}^{n,*}) \mathbf{W}^{n,*})| \leq C (\|\mathbf{V}^{n-1} - \mathbf{W}^{n-1}\|_1 + \|\mathbf{y}^{n-1} - \mathbf{z}^{n-1}\|_\infty), \quad (5.4)$$

$1 \leq j \leq J + n, 1 \leq n \leq N - 1$.

Proof. From (3.9), by means of hypothesis (H6) and inequality (5.1), we obtain the first inequality, Q4 1

$$\begin{aligned} |y_j^{n,*} - z_j^{n,*}| &\leq |y_{j-1}^{n-1} - z_{j-1}^{n-1}| + k |g(y_{j-1}^{n-1}, \mathcal{Q}_{j-1}^{n-1}(\mathbf{y}^{n-1}, \boldsymbol{\gamma}(\mathbf{y}^{n-1}) \mathbf{V}^{n-1}), t_{n-1}) \\ &\quad - g(z_{j-1}^{n-1}, \mathcal{Q}_{j-1}^{n-1}(\mathbf{z}^{n-1}, \boldsymbol{\gamma}(\mathbf{z}^{n-1}) \mathbf{W}^{n-1}), t_{n-1})| \\ &\leq (1 + Ck) |y_{j-1}^{n-1} - z_{j-1}^{n-1}| + Ck |\mathcal{Q}_{j-1}^{n-1}(\mathbf{y}^{n-1}, \boldsymbol{\gamma}(\mathbf{y}^{n-1}) \mathbf{V}^{n-1}) - \mathcal{Q}_{j-1}^{n-1}(\mathbf{z}^{n-1}, \boldsymbol{\gamma}(\mathbf{z}^{n-1}) \mathbf{W}^{n-1})| \\ &\leq (1 + Ck) |y_{j-1}^{n-1} - z_{j-1}^{n-1}| + Ck \{ \|\mathbf{y}^{n-1} - \mathbf{z}^{n-1}\|_\infty + \|\mathbf{V}^{n-1} - \mathbf{W}^{n-1}\|_1 \}, \end{aligned} \quad (5.5)$$

$1 \leq j \leq J + n$, $1 \leq n \leq N$. Now, from (3.10), we obtain 6

$$\begin{aligned} |y_j^{n,*} - W_j^{n,*}| &\leq |V_{j-1}^{n-1} - W_{j-1}^{n-1}| \exp(-km(y_{j-1}^{n-1}, \mathcal{Q}_{j-1}^{n-1}(\mathbf{y}^{n-1}, \boldsymbol{\gamma}(\mathbf{y}^{n-1}) \mathbf{V}^{n-1}), V_{j-1}^{n-1}, t_{n-1})) \\ &\quad + |W_{j-1}^{n-1}| |\exp(-km(y_{j-1}^{n-1}, \mathcal{Q}_{j-1}^{n-1}(\mathbf{y}^{n-1}, \boldsymbol{\gamma}(\mathbf{y}^{n-1}) \mathbf{V}^{n-1}), V_{j-1}^{n-1}, t_{n-1})) \\ &\quad - \exp(-km(z_{j-1}^{n-1}, \mathcal{Q}_{j-1}^{n-1}(\mathbf{z}^{n-1}, \boldsymbol{\gamma}(\mathbf{z}^{n-1}) \mathbf{W}^{n-1}), W_{j-1}^{n-1}, t_{n-1}))|, \end{aligned} \quad (5.6)$$

$1 \leq j \leq J + n$. Next, by means of hypotheses (H1)–(H6), we have 10

$$\exp(-km(y_{j-1}^{n-1}, \mathcal{Q}_{j-1}^{n-1}(\mathbf{y}^{n-1}, \boldsymbol{\gamma}(\mathbf{y}^{n-1}) \mathbf{V}^{n-1}), V_{j-1}^{n-1}, t_{n-1})) \leq 1 + Ck, \quad (5.7) \quad 11$$

$1 \leq j \leq J + n$. Therefore, hypotheses (H1)–(H6), inequalities (5.6)–(5.7) and (5.1), and $\|\mathbf{W}^n\|_\infty \leq C$ allow us to obtain 12

$$\begin{aligned} |y_j^{n,*} - W_j^{n,*}| &\leq (1 + Ck) |V_{j-1}^{n-1} - W_{j-1}^{n-1}| + Ck |m(y_{j-1}^{n-1}, \mathcal{Q}_{j-1}^{n-1}(\mathbf{y}^{n-1}, \boldsymbol{\gamma}(\mathbf{y}^{n-1}) \mathbf{V}^{n-1}), V_{j-1}^{n-1}, t_{n-1}) \\ &\quad - m(z_{j-1}^{n-1}, \mathcal{Q}_{j-1}^{n-1}(\mathbf{z}^{n-1}, \boldsymbol{\gamma}(\mathbf{z}^{n-1}) \mathbf{W}^{n-1}), W_{j-1}^{n-1}, t_{n-1})| \\ &\leq (1 + Ck) |V_{j-1}^{n-1} - W_{j-1}^{n-1}| + Ck \|\mathbf{y}^{n-1} - \mathbf{z}^{n-1}\|_\infty + Ck \|\mathbf{V}^{n-1} - \mathbf{W}^{n-1}\|_1, \end{aligned} \quad (5.8) \quad 15$$

$1 \leq j \leq J + n$, $1 \leq n \leq N$, which proves the second inequality. 16

The triangle inequality, hypotheses (H2), inequalities (5.2)–(5.3) and that $\|\mathbf{W}^{n,*}\|_\infty \leq C$ yield 17

$$\begin{aligned} |\mathcal{Q}_j^n(\mathbf{y}^{n,*}, \boldsymbol{\gamma}(\mathbf{y}^{n,*}) \mathbf{V}^{n,*}) - \mathcal{Q}_j^n(\mathbf{z}^{n,*}, \boldsymbol{\gamma}(\mathbf{z}^{n,*}) \mathbf{W}^{n,*})| &\leq (1 + Ck) \|\mathbf{V}^{n-1} - \mathbf{W}^{n-1}\|_1 + (1 + Ck) \|\mathbf{y}^{n-1} - \mathbf{z}^{n-1}\|_\infty \\ &\leq C (\|\mathbf{V}^{n-1} - \mathbf{W}^{n-1}\|_1 + \|\mathbf{y}^{n-1} - \mathbf{z}^{n-1}\|_\infty), \end{aligned} \quad 18$$

$1 \leq j \leq J + n$, $1 \leq n \leq N - 1$, as desired. \square 19

Next, we introduce the theorem that establishes the stability of the discretization defined by the Eqs. (3.4)–(3.8). 20

Theorem 3. Let us assume that hypotheses (H1)–(H6) about problem (1.1)–(1.4), and properties (P1)–(P6) of the quadrature rule hold. Then, the discretization is stable for $\tilde{\mathbf{u}}_h$ with $R_h = Rh^p$, $1 < p < 2$. 21

Proof. We denote 22

$$\Phi_h(\mathbf{y}^0, \mathbf{V}^0, \mathbf{y}^1, \mathbf{V}^1, \dots, \mathbf{y}^N, \mathbf{V}^N) = (\mathbf{Y}^0, \mathbf{P}^0, \mathbf{P}_0, \mathbf{Y}^1, \mathbf{P}^1, \dots, \mathbf{Y}^N, \mathbf{P}^N), \quad 25$$

$$\Phi_h(\mathbf{z}^0, \mathbf{W}^0, \mathbf{z}^1, \mathbf{W}^1, \dots, \mathbf{z}^N, \mathbf{W}^N) = (\mathbf{Z}^0, \mathbf{L}^0, \mathbf{L}_0, \mathbf{Z}^1, \mathbf{L}^1, \dots, \mathbf{Z}^N, \mathbf{L}^N), \quad 26$$

$(\mathbf{y}^0, \mathbf{V}^0, \mathbf{y}^1, \mathbf{V}^1, \dots, \mathbf{y}^N, \mathbf{V}^N), (\mathbf{z}^0, \mathbf{W}^0, \mathbf{z}^1, \mathbf{W}^1, \dots, \mathbf{z}^N, \mathbf{W}^N) \in B_{\mathcal{A}_h}(\tilde{\mathbf{u}}_h, L_h)$. Now, we set 27

$$\mathbf{E}^n = \mathbf{V}^n - \mathbf{W}^n \in \mathbb{R}^{J+n}, \quad \Delta^n = \mathbf{y}^n - \mathbf{z}^n \in \mathbb{R}^{J+n-1}, \quad 0 \leq n \leq N. \quad 28$$

By means of (3.7), hypotheses (H1)–(H6), and inequalities (5.1)–(5.2), (5.4) yield 29

$$\begin{aligned} |\Delta_j^n| &\leq |\Delta_{j-1}^{n-1}| + k |Y_j^n - Z_j^n| \\ &\quad + \frac{k}{2} |g(y_{j-1}^{n-1}, \mathcal{Q}_{j-1}^{n-1}(\mathbf{y}^{n-1}, \boldsymbol{\gamma}(\mathbf{y}^{n-1}) \mathbf{V}^{n-1}), t_{n-1}) - g(z_{j-1}^{n-1}, \mathcal{Q}_{j-1}^{n-1}(\mathbf{z}^{n-1}, \boldsymbol{\gamma}(\mathbf{z}^{n-1}) \mathbf{W}^{n-1}), t_{n-1})| \\ &\quad + \frac{k}{2} |g(y_j^{n,*}, \mathcal{Q}_j^n(\mathbf{y}^{n,*}, \boldsymbol{\gamma}(\mathbf{y}^{n,*}) \mathbf{V}^{n,*}), t_n) - g(z_j^{n,*}, \mathcal{Q}_j^n(\mathbf{z}^{n,*}, \boldsymbol{\gamma}(\mathbf{z}^{n,*}) \mathbf{W}^{n,*}), t_n)| \\ &\leq |\Delta_{j-1}^{n-1}| + k |Y_j^n - Z_j^n| + Ck |y_{j-1}^{n-1} - z_{j-1}^{n-1}| + Ck |y_j^{n,*} - z_j^{n,*}| \\ &\quad + Ck |\mathcal{Q}_{j-1}^{n-1}(\mathbf{y}^{n-1}, \boldsymbol{\gamma}(\mathbf{y}^{n-1}) \mathbf{V}^{n-1}) - \mathcal{Q}_{j-1}^{n-1}(\mathbf{z}^{n-1}, \boldsymbol{\gamma}(\mathbf{z}^{n-1}) \mathbf{W}^{n-1})| \\ &\quad + Ck |\mathcal{Q}_j^n(\mathbf{y}^{n,*}, \boldsymbol{\gamma}(\mathbf{y}^{n,*}) \mathbf{V}^{n,*}) - \mathcal{Q}_j^n(\mathbf{z}^{n,*}, \boldsymbol{\gamma}(\mathbf{z}^{n,*}) \mathbf{W}^{n,*})| \\ &\leq |\Delta_{j-1}^{n-1}| + k |Y_j^n - Z_j^n| + Ck \{ \|\Delta^{n-1}\|_\infty + \|\mathbf{E}^{n-1}\|_1 \} + Ck \{ (1 + Ck) |\Delta_{j-1}^{n-1}| + Ck \|\Delta^{n-1}\|_\infty + Ck \|\mathbf{E}^{n-1}\|_1 \} \\ &\leq |\Delta_{j-1}^{n-1}| + k |Y_j^n - Z_j^n| + Ck \{ \|\Delta^{n-1}\|_\infty + \|\mathbf{E}^{n-1}\|_1 \}, \end{aligned} \quad (5.9) \quad 37$$

$1 \leq j \leq J + n - 1$, $1 \leq n \leq N$. 38

Thus, when $N \geq n > j \geq 1$, from (5.9), we have

$$|\Delta_j^n| \leq C k \sum_{l=0}^{j-1} \{ \|\mathbf{E}^{n-1-l}\|_1 + \|\Delta^{n-1-l}\|_\infty \} + k \sum_{l=0}^{j-1} |Y_{j-l}^{n-l} - Z_{j-l}^{n-l}|. \quad (5.10)$$

Therefore, when $N \geq n > j \geq 1$, by means of (5.10), we establish

$$|\Delta_j^n| \leq C \left\{ \sum_{m=n-j}^{n-1} k \|\mathbf{E}^m\|_1 + \sum_{m=n-j}^{n-1} k \|\Delta^m\|_\infty \right\} + \sum_{m=n-j+1}^n k \|\mathbf{Y}^m - \mathbf{Z}^m\|_\infty. \quad (5.11)$$

On the other hand, when $J + n - 1 \geq j \geq n \geq 1$, due to (5.9) it follows

$$|\Delta_j^n| \leq |\Delta_{j-n}^0| + C k \sum_{l=0}^{n-1} \left\{ \|\mathbf{E}^{n-1-l}\|_1 + \|\Delta^{n-1-l}\|_\infty + k \sum_{l=0}^{n-1} |Y_{j-l}^{n-l} - Z_{j-l}^{n-l}| \right\}. \quad (5.12)$$

Thus, when $J + n - 1 \geq j \geq n \geq 1$, (5.12) yields

$$|\Delta_j^n| \leq \|\Delta^0\|_\infty + C \left\{ \sum_{m=0}^{n-1} k \|\mathbf{E}^m\|_1 + \sum_{m=0}^{n-1} k \|\Delta^m\|_\infty \right\} + \sum_{m=1}^n k \|\mathbf{Y}^m - \mathbf{Z}^m\|_\infty. \quad (5.13)$$

Then, by means of (5.11) and (5.13), we can conclude that

$$\|\Delta^n\|_\infty \leq \|\Delta^0\|_\infty + C \left\{ \sum_{m=0}^{n-1} k \|\mathbf{E}^m\|_1 + \sum_{m=0}^{n-1} k \|\Delta^m\|_\infty \right\} + \sum_{m=1}^n k \|\mathbf{Y}^m - \mathbf{Z}^m\|_\infty, \quad (5.14)$$

$1 \leq n \leq N$.

On the other hand, from (3.8) we arrive at

$$\begin{aligned} |E_j^n| &\leq |E_{j-1}^{n-1}| \exp \left\{ -\frac{k}{2} (m(y_{j-1}^{n-1}, \mathcal{Q}_{j-1}^{n-1}(\mathbf{y}^{n-1}, \boldsymbol{\gamma}(\mathbf{y}^{n-1}) \mathbf{V}^{n-1}), V_{j-1}^{n-1}, t_{n-1})) \right. \\ &\quad \left. + m(y_j^{n,*}, \mathcal{Q}_j^n(\mathbf{y}^{n,*}, \boldsymbol{\gamma}(\mathbf{y}^{n,*}) \mathbf{V}^{n,*}), V_j^{n,*}, t_n) \right\} \\ &\quad + |W_{j-1}^{n-1}| \left| \exp \left\{ -\frac{k}{2} (m(y_{j-1}^{n-1}, \mathcal{Q}_{j-1}^{n-1}(\mathbf{y}^{n-1}, \boldsymbol{\gamma}(\mathbf{y}^{n-1}) \mathbf{V}^{n-1}), V_{j-1}^{n-1}, t_{n-1})) \right. \right. \\ &\quad \left. \left. + m(y_j^{n,*}, \mathcal{Q}_j^n(\mathbf{y}^{n,*}, \boldsymbol{\gamma}(\mathbf{y}^{n,*}) \mathbf{V}^{n,*}), V_j^{n,*}, t_n) \right\} \right. \\ &\quad \left. - \exp \left\{ -\frac{k}{2} (m(z_{j-1}^{n-1}, \mathcal{Q}_{j-1}^{n-1}(\mathbf{z}^{n-1}, \boldsymbol{\gamma}(\mathbf{z}^{n-1}) \mathbf{W}^{n-1}), W_{j-1}^{n-1}, t_{n-1})) \right. \right. \\ &\quad \left. \left. + m(z_j^{n,*}, \mathcal{Q}_j^n(\mathbf{z}^{n,*}, \boldsymbol{\gamma}(\mathbf{z}^{n,*}) \mathbf{W}^{n,*}), W_j^{n,*}, t_n) \right\} \right| + k |P_j^n - L_j^n|, \end{aligned} \quad (5.15)$$

$1 \leq j \leq J + n - 1$, $1 \leq n \leq N$. Now, by means of hypotheses (H4) and (H6), we have

$$\begin{aligned} &\exp \left\{ -\frac{k}{2} (m(y_{j-1}^{n-1}, \mathcal{Q}_{j-1}^{n-1}(\mathbf{y}^{n-1}, \boldsymbol{\gamma}(\mathbf{y}^{n-1}) \mathbf{V}^{n-1}), V_{j-1}^{n-1}, t_{n-1})) + m(y_j^{n,*}, \mathcal{Q}_j^n(\mathbf{y}^{n,*}, \boldsymbol{\gamma}(\mathbf{y}^{n,*}) \mathbf{V}^{n,*}), V_j^{n,*}, t_n) \right\} \\ &\leq 1 + C k, \end{aligned} \quad (5.16)$$

$1 \leq j \leq J + n - 1$, $1 \leq n \leq N$. Thus, with (5.1)–(5.4), (5.15)–(5.16), hypotheses (H4) and (H6), and that $\|\mathbf{W}^{n-1}\|_\infty \leq C$, we obtain

$$\begin{aligned} |E_j^n| &\leq k |P_j^n - L_j^n| + (1 + C k) |E_{j-1}^{n-1}| + C k \left| m(y_{j-1}^{n-1}, \mathcal{Q}_{j-1}^{n-1}(\mathbf{y}^{n-1}, \boldsymbol{\gamma}(\mathbf{y}^{n-1}) \mathbf{V}^{n-1}), V_{j-1}^{n-1}, t_{n-1}) \right. \\ &\quad \left. - m(z_{j-1}^{n-1}, \mathcal{Q}_{j-1}^{n-1}(\mathbf{z}^{n-1}, \boldsymbol{\gamma}(\mathbf{z}^{n-1}) \mathbf{W}^{n-1}), W_{j-1}^{n-1}, t_{n-1}) \right| + C k \left| m(y_j^{n,*}, \mathcal{Q}_j^n(\mathbf{y}^{n,*}, \boldsymbol{\gamma}(\mathbf{y}^{n,*}) \mathbf{V}^{n,*}), V_j^{n,*}, t_n) \right. \\ &\quad \left. - m(z_j^{n,*}, \mathcal{Q}_j^n(\mathbf{z}^{n,*}, \boldsymbol{\gamma}(\mathbf{z}^{n,*}) \mathbf{W}^{n,*}), W_j^{n,*}, t_n) \right| \\ &\leq k |P_j^n - L_j^n| + (1 + C k) |E_{j-1}^{n-1}| + C k (\|\mathbf{E}^{n-1}\|_1 + \|\Delta^{n-1}\|_\infty), \end{aligned} \quad (5.17)$$

$1 \leq j \leq J + n - 1, 1 \leq n \leq N$. Now, from (3.6) and hypothesis (H6) it follows

$$\begin{aligned} |E_0^n| &\leq \left| \frac{\mathcal{Q}_0^n(\mathbf{y}^n, \boldsymbol{\alpha}(\mathbf{y}^n, \mathbf{V}^n) \mathbf{V}^n)}{g(x_m, \mathcal{Q}_j^n(\mathbf{y}^n, \boldsymbol{\gamma}(\mathbf{y}^n) \mathbf{V}^n), t_n)} - \frac{\mathcal{Q}_0^n(\mathbf{z}^n, \boldsymbol{\alpha}(\mathbf{z}^n, \mathbf{W}^n) \mathbf{W}^n)}{g(x_m, \mathcal{Q}_j^n(\mathbf{z}^n, \boldsymbol{\gamma}(\mathbf{z}^n) \mathbf{W}^n), t_n)} \right| + |P_0^n - L_0^n| \\ &\leq C \left| g(x_m, \mathcal{Q}_j^n(\mathbf{z}^n, \boldsymbol{\gamma}(\mathbf{z}^n) \mathbf{W}^n), t_n) - g(x_m, \mathcal{Q}_j^n(\mathbf{y}^n, \boldsymbol{\gamma}(\mathbf{y}^n) \mathbf{V}^n), t_n) \right| |\mathcal{Q}_0^n(\mathbf{y}^n, \boldsymbol{\alpha}(\mathbf{y}^n, \mathbf{V}^n) \mathbf{V}^n)| \\ &\quad + \left| g(x_m, \mathcal{Q}_j^n(\mathbf{y}^n, \boldsymbol{\gamma}(\mathbf{y}^n) \mathbf{V}^n), t_n) \right| |\mathcal{Q}_0^n(\mathbf{y}^n, \boldsymbol{\alpha}(\mathbf{y}^n, \mathbf{V}^n) \mathbf{V}^n) - \mathcal{Q}_0^n(\mathbf{z}^n, \boldsymbol{\alpha}(\mathbf{z}^n, \mathbf{W}^n) \mathbf{W}^n)| + |P_0^n - L_0^n|, \end{aligned} \quad (5.18)$$

$1 \leq n \leq N$. Next, with hypotheses (H5) and $\|\mathbf{W}^n\|_\infty \leq C$, we arrive at

$$|\mathcal{Q}_0^n(\mathbf{y}^n, \boldsymbol{\alpha}(\mathbf{y}^n, \mathbf{V}^n) \mathbf{V}^n)| \leq C, \quad (5.19)$$

Q5 $1 \leq n \leq N$. Furthermore, the definition of α_j , hypotheses (H5) and Proposition 2 yield

$$\begin{aligned} |\alpha_j(\mathbf{y}^n, \mathbf{V}^n) - \alpha_j(\mathbf{z}^n, \mathbf{W}^n)| &\leq |\alpha(\mathbf{y}_j^n, \mathcal{Q}_j^n(\mathbf{y}^n, \boldsymbol{\gamma}(\mathbf{y}^n) \mathbf{V}^n), t_n) - \alpha(\mathbf{z}_j^n, \mathcal{Q}_j^n(\mathbf{y}^n, \boldsymbol{\gamma}(\mathbf{y}^n) \mathbf{V}^n), t_n)| \\ &\quad + |\alpha(\mathbf{z}_j^n, \mathcal{Q}_j^n(\mathbf{y}^n, \boldsymbol{\gamma}(\mathbf{y}^n) \mathbf{V}^n), t_n) - \alpha(\mathbf{z}_j^n, \mathcal{Q}_j^n(\mathbf{z}^n, \boldsymbol{\gamma}(\mathbf{z}^n) \mathbf{W}^n), t_n)| \\ &\leq C \{ |\Delta_j^n| + \|\Delta^n\|_\infty + \|\mathbf{E}^n\|_1 \}, \end{aligned} \quad (5.20)$$

$0 \leq j \leq J + n - 1, 1 \leq n \leq N$.

Next, by means of (5.20), hypotheses (H5), property (P6) and $\|\mathbf{W}^n\|_\infty \leq C$, we arrive at

$$\begin{aligned} |\mathcal{Q}_0^n(\mathbf{y}^n, \boldsymbol{\alpha}(\mathbf{y}^n, \mathbf{V}^n) \mathbf{V}^n) - \mathcal{Q}_0^n(\mathbf{z}^n, \boldsymbol{\alpha}(\mathbf{z}^n, \mathbf{W}^n) \mathbf{W}^n)| &\leq |\mathcal{Q}_0^n(\mathbf{y}^n, \boldsymbol{\alpha}(\mathbf{y}^n, \mathbf{V}^n) \mathbf{V}^n) - \mathcal{Q}_0^n(\mathbf{z}^n, \boldsymbol{\alpha}(\mathbf{y}^n, \mathbf{V}^n) \mathbf{V}^n)| \\ &\quad + |\mathcal{Q}_0^n(\mathbf{z}^n, (\boldsymbol{\alpha}(\mathbf{y}^n, \mathbf{V}^n) - \boldsymbol{\alpha}(\mathbf{z}^n, \mathbf{W}^n)) \mathbf{V}^n)| \\ &\quad + |\mathcal{Q}_0^n(\mathbf{z}^n, \boldsymbol{\alpha}(\mathbf{z}^n, \mathbf{W}^n) (\mathbf{V}^n - \mathbf{W}^n))| \\ &\leq C \{ \|\mathbf{E}^n\|_1 + \|\Delta^n\|_\infty \}, \end{aligned} \quad (5.21)$$

$1 \leq n \leq N$. Therefore, we complete the derivation of the stability estimate for the boundary node taking into account (5.18)–(5.19) and (5.21), hypothesis (H6) and Proposition 2, ▲

$$|E_0^n| \leq |P_0^n - L_0^n| + C \{ \|\Delta^n\|_\infty + \|\mathbf{E}^n\|_1 \}, \quad (5.22)$$

$1 \leq n \leq N$.

Thus, when $N \geq n > j \geq 1$, from (5.17), we obtain

$$|E_j^n| \leq (1 + Ck)^j |E_0^{n-j}| + k \sum_{l=0}^{j-1} (1 + Ck)^l |P_{j-l}^{n-l} - L_{j-l}^{n-l}| + Ck \sum_{l=0}^{j-1} (1 + Ck)^l \{ \|\mathbf{E}^{n-1-l}\|_1 + \|\Delta^{n-1-l}\|_\infty \}. \quad (5.23)$$

Therefore, we establish

$$|E_j^n| \leq C \left\{ |E_0^{n-j}| + \sum_{m=n-j}^{n-1} k \|\mathbf{E}^m\|_1 + \sum_{m=n-j}^{n-1} k \|\Delta^m\|_\infty + \sum_{m=n-j+1}^n k \|\mathbf{P}^m - \mathbf{L}^m\|_\infty \right\}. \quad (5.24)$$

On the other hand, when $J + n - 1 \geq j \geq n \geq 1$, due to (5.17) it follows

$$|E_j^n| \leq (1 + Ck)^n |E_{j-n}^0| + k \sum_{l=0}^{n-1} (1 + Ck)^l |P_{j-l}^{n-l} - L_{j-l}^{n-l}| + Ck \sum_{l=0}^{n-1} (1 + Ck)^l \{ \|\mathbf{E}^{n-1-l}\|_1 + \|\Delta^{n-1-l}\|_\infty \}. \quad (5.25)$$

Thus, we can conclude

$$|E_j^n| \leq C \left\{ |E_{j-n}^0| + \sum_{m=0}^{n-1} k \|\mathbf{E}^m\|_1 + \sum_{m=0}^{n-1} k \|\Delta^m\|_\infty + \sum_{m=1}^n k \|\mathbf{P}^m - \mathbf{L}^m\|_\infty \right\}. \quad (5.26)$$

Now, multiplying $|E_j^n|$ by h and summing in j , $0 \leq j \leq J + n - 1, 1 \leq n \leq N$, from (5.22), (5.24) and (5.26) and that $k = r h$, we have

$$\begin{aligned} \|\mathbf{E}^n\|_1 &= h |E_0^n| + \sum_{j=1}^{n-1} h |E_j^n| + \sum_{j=n}^{J+n-1} h |E_j^n| \\ &\leq h |P_0^n - L_0^n| + Ch (\|\mathbf{E}^n\|_1 + \|\Delta^n\|_\infty) \\ &\leq C \left\{ \|\mathbf{E}^0\|_1 + \sum_{j=1}^{n-1} h |E_0^{n-j}| + h \|\mathbf{E}^n\|_1 + \sum_{m=0}^{n-1} k \|\mathbf{E}^m\|_1 \right\} \end{aligned}$$

$$\begin{aligned}
& + h \|\Delta^n\|_\infty + \sum_{m=0}^{n-1} k \|\Delta^m\|_\infty + \sum_{m=1}^n k \|\mathbf{P}^m - \mathbf{L}^m\|_\infty + h |P_0^n - L_0^n| \Big\} \\
& \leq C \left\{ \|\mathbf{E}^0\|_1 + \sum_{m=0}^n k \|\mathbf{E}^m\|_1 + \sum_{m=0}^n k \|\Delta^m\|_\infty + \sum_{m=1}^n k \|\mathbf{P}^m - \mathbf{L}^m\|_\infty + \sum_{m=1}^n h |P_0^m - L_0^m| \right\},
\end{aligned}$$

$1 \leq n \leq N$. Then

$$\|\mathbf{E}^n\|_1 \leq C \left\{ \|\mathbf{E}^0\|_1 + \sum_{m=1}^n k \|\mathbf{E}^m\|_1 + \sum_{m=0}^n k \|\Delta^m\|_\infty + \sum_{m=1}^n k \|\mathbf{P}^m - \mathbf{L}^m\|_\infty + \|\mathbf{P}_0 - \mathbf{L}_0\|_\infty \right\}, \quad (5.27)$$

$1 \leq n \leq N$. Thus, by means of the discrete Gronwall Lemma,

$$\|\mathbf{E}^n\|_1 \leq C \left\{ \|\mathbf{E}^0\|_1 + \sum_{m=0}^n k \|\Delta^m\|_\infty + \sum_{m=1}^n k \|\mathbf{P}^m - \mathbf{L}^m\|_\infty + \|\mathbf{P}_0 - \mathbf{L}_0\|_\infty \right\}, \quad (5.28)$$

$1 \leq n \leq N$. Next, we substitute (5.28) in (5.14) to have

$$\|\Delta^n\|_\infty \leq C \left\{ \|\Delta^0\|_\infty + \|\mathbf{E}^0\|_1 + \sum_{m=1}^{n-1} k \|\Delta^m\|_\infty + \sum_{m=1}^n k \|\mathbf{Y}^m - \mathbf{Z}^m\|_\infty + \sum_{m=1}^{n-1} k \|\mathbf{P}^m - \mathbf{L}^m\|_\infty + \|\mathbf{P}_0 - \mathbf{L}_0\|_\infty \right\}, \quad (5.29)$$

$1 \leq n \leq N$. Again, by means of the discrete Gronwall Lemma, it follows

$$\|\Delta^n\|_\infty \leq C \left\{ \|\Delta^0\|_\infty + \|\mathbf{E}^0\|_1 + \|\mathbf{P}_0 - \mathbf{L}_0\|_\infty + \sum_{m=1}^{n-1} k \|\mathbf{P}^m - \mathbf{L}^m\|_\infty + \sum_{m=1}^n k \|\mathbf{Y}^m - \mathbf{Z}^m\|_\infty \right\}, \quad (5.30)$$

$1 \leq n \leq N$. Next, we substitute (5.30) in (5.28) to obtain

$$\|\mathbf{E}^n\|_1 \leq C \left\{ \|\Delta^0\|_\infty + \|\mathbf{E}^0\|_1 + \|\mathbf{P}_0 - \mathbf{L}_0\|_\infty + \sum_{m=1}^n k \|\mathbf{P}^m - \mathbf{L}^m\|_\infty + \sum_{m=1}^n k \|\mathbf{Y}^m - \mathbf{Z}^m\|_\infty \right\}, \quad (5.31)$$

$1 \leq n \leq N$. And, finally, we substitute (5.30)–(5.31) in (5.22), (5.24) and (5.26) to arrive at

$$\|\mathbf{E}^n\|_\infty \leq C \left\{ \|\Delta^0\|_\infty + \|\mathbf{E}^0\|_1 + \|\mathbf{P}_0 - \mathbf{L}_0\|_\infty + \sum_{m=1}^n k \|\mathbf{P}^m - \mathbf{L}^m\|_\infty + \sum_{m=1}^n k \|\mathbf{Y}^m - \mathbf{Z}^m\|_\infty \right\}, \quad (5.32)$$

$1 \leq n \leq N$. Thus, due to (5.30) and (5.32) we have

$$\begin{aligned}
& \|(\Delta^0, \mathbf{E}^0, \dots, \Delta^N, \mathbf{E}^N)\|_{\mathcal{A}_h} \\
& \leq C \|(\Delta^0, \mathbf{E}^0, \mathbf{P}_0 - \mathbf{L}_0, \mathbf{Y}^1 - \mathbf{Z}^1, \mathbf{P}^1 - \mathbf{L}^1, \dots, \mathbf{Y}^N - \mathbf{Z}^N, \mathbf{P}^N - \mathbf{L}^N)\|_{\mathcal{B}_h}. \quad \square
\end{aligned}$$

6. Convergence

The global discretization error is defined as

$$\tilde{\mathbf{e}}_h = \tilde{\mathbf{u}}_h - \tilde{\mathbf{U}}_h \in \mathcal{A}_h.$$

We say that the discretization (3.3) is convergent if there exists $h_0 > 0$ such that, for each $h \in H$ with $h \leq h_0$, (3.11) has a solution $\tilde{\mathbf{U}}_h$ for which, as $h \rightarrow 0$,

$$\lim \|\tilde{\mathbf{u}}_h - \tilde{\mathbf{U}}_h\|_{\mathcal{A}_h} = \lim \|\tilde{\mathbf{e}}_h\|_{\mathcal{A}_h} = 0.$$

In our analysis, we shall use the following result of the general discretization framework introduced by López-Marcos et al. [26].

Theorem 4. Let us assume that (3.3) is consistent and stable with thresholds R_h . If Φ_h is continuous in $B(\tilde{\mathbf{u}}_h, R_h)$ and $\|\mathbf{l}_h\|_{\mathcal{B}_h} = o(R_h)$ as $h \rightarrow 0$, then:

- (i) For h sufficiently small, the discrete equations (3.11) possess a unique solution in $B(\tilde{\mathbf{u}}_h, R_h)$.
- (ii) As $h \rightarrow 0$, the solutions converge and $\|\tilde{\mathbf{e}}_h\|_{\mathcal{A}_h} = O(\|\mathbf{l}_h\|_{\mathcal{B}_h})$.

Finally, we posit the following theorem that establishes the convergence of the numerical method defined by Eqs. (3.4)–(3.8).

Theorem 5. Let us assume that hypotheses (H1)–(H6) about problem (1.1)–(1.4) hold, and that the considered quadrature rules satisfy properties (P1)–(P6). Then, for h sufficiently small, the numerical method defined by Eqs. (3.4)–(3.8) has a unique solution $\tilde{\mathbf{U}}_h \in B(\tilde{\mathbf{u}}_h, R_h)$ and

$$\|\tilde{\mathbf{U}}_h - \tilde{\mathbf{u}}_h\|_{\mathcal{A}_h} \leq C (\|\mathbf{x}^0 - \mathbf{X}^0\|_\infty + \|\mathbf{u}^0 - \mathbf{U}^0\|_\infty + O(h^2 + k^2)). \quad (6.1)$$

The proof of Theorem 5 is derived by means of consistency (Theorem 2), stability (Theorem 3) and Theorem 4.

Next, we can establish an error bound for the numerical and the theoretical solution at the numerical values of the grid nodes.

Theorem 6. Let us assume that hypotheses (H1)–(H6) about problem (1.1)–(1.4) hold, and that the considered quadrature rules satisfy properties (P1)–(P6). For h sufficiently small, let $\mathbf{u}_h^* = (\mathbf{u}_*^0, \mathbf{u}_*^1, \mathbf{u}_*^2, \dots, \mathbf{u}_*^N) \in \prod_{n=0}^N \mathbb{R}^{J+n}$, defined by

$$\mathbf{u}_*^n = (u(X_0^n, t_n), u(X_1^n, t_n), \dots, u(X_{J+n-1}^n, t_n)) \in \mathbb{R}^{J+n},$$

$0 \leq n \leq N$, where X_j^n , $0 \leq j \leq J+n-1$, $0 \leq n \leq N$, are the grid nodes given by scheme (3.4)–(3.8). Then,

$$\|\mathbf{U}^n - \mathbf{u}_*^n\|_\infty \leq C (\|\mathbf{x}^0 - \mathbf{X}^0\|_\infty + \|\mathbf{u}^0 - \mathbf{U}^0\|_\infty + O(h^2 + k^2)). \quad (6.2)$$

This theorem follows immediately from Theorem 5. In particular, if $\mathbf{X}^0 = \mathbf{x}^0$ and $\mathbf{U}^0 = \mathbf{u}^0$, the proposed numerical scheme is second-order accurate.

At this moment, we have obtained the convergence of the numerical method (2.14)–(2.19) which does not employ selection at each time level. Also, we have proved the convergence of numerical methods which employ a selection criteria, whenever the positions, which are determined by the criteria we have chosen, lead us to subgrids which satisfy the property (SG). For the criteria presented in this paper, this property could be shown in two stages. First, as proved in [25], for the selection criteria given in (2.20), it leads us to subgrids with such a property, when we applied it over nodes which are in a neighbourhood of the theoretical ones with radius Rh^p (for criteria (2.21) we could prove the same in a similar way). In a second stage, it is proved that the nodes, which in fact the numerical method computes, are in such neighbourhoods. In order to do this, it is enough to realize that such nodes could be seen, up to each level of time, as the solutions obtained by a discrete operator which has the form of the one defined in (3.3).

With respect to the convergence behaviour of these kind of numerical schemes when the theoretical solution has weak singularities, we refer to the corresponding section of [25] because for both equations and numerical methods the behaviour along characteristics curves are similar.

7. Numerical results

We have carried out numerical experiments with the scheme defined in Section 2. We have considered a theoretical test problem that presents meaningful nonlinearities (both from a mathematical and biological point of view). The numerical integration for the numerical experiment was carried out on the time interval $[0, 10]$. The size interval was taken as $[0, 1]$.

The size-specific growth, fertility and mortality moduli are chosen as $g(x, z, t) = \frac{1-x}{1+z}$, $\alpha(x, z, t) = \frac{x(1-x)}{2(z+1)}$,

$$\mu(x, z, t) = \frac{2(1+z)}{1 + \frac{1}{2}e^{-2t} \left((1-x)^2 + (1-x) \sqrt{(1-x)^2 + 4e^{2t}} \right)}.$$

The weight function is taken as $\gamma(x) = 1$ (we consider the total population) and the external inflow function as

$$\Gamma(t) = e^{-2t} \frac{1 + \frac{1+2e^{2t}}{\sqrt{1+4e^{2t}}}}{1 + \frac{e^{-2t}}{2} (1 + \sqrt{1+4e^{2t}})} + 2e^t - \frac{\sqrt{1+4e^{2t}}}{2} - 2e^{2t} \log \left(\frac{e^{-t}}{2} (1 + \sqrt{1+4e^{2t}}) \right).$$

Finally, we consider as the initial size-specific density the function

$$u_0(x) = (1-x) + \frac{(1-x)^2 + 2}{\sqrt{(1-x)^2 + 4}}.$$

With the functions chosen, the problem (1.1)–(1.4) has the following solution

$$u(x, t) = e^{-2t} \left((1-x) + \frac{(1-x)^2 + 2e^{2t}}{\sqrt{(1-x)^2 + 4e^{2t}}} \right).$$

Since we know the exact solution to each problem, we can show numerically that our methods are second-order accurate by means of error tables. In Tables 2–4, we present the results obtained for the test problem with the three different selection procedures.

Table 2
Error and experimental order of convergence. Method without selection.

k	h				
	3.125e-2	1.563e-2	7.813e-3	3.906e-3	1.953e-3
3.125e-2	1.585e-4	8.297e-5	8.456e-5	8.496e-5	8.506e-5
1.563e-2	1.580e-4	4.223e-5 1.908	2.069e-5 2.004	2.109e-5 2.004	2.119e-5 2.004
7.813e-3	1.581e-4	4.033e-5 1.970	1.089e-5 1.955	5.166e-6 2.002	5.265e-6 2.002
3.906e-3	1.586e-4	3.987e-5 1.987	1.019e-5 1.985	2.766e-6 1.977	1.291e-6 2.001
1.953e-3	1.590e-4	3.982e-5 1.994	1.001e-5 1.994	2.560e-6 1.993	6.970e-7 1.989

Table 3
Error and experimental order of convergence. Method with selection (2.21) (constant number of grid nodes).

k	h				
	3.125e-2	1.563e-2	7.813e-3	3.906e-3	1.953e-3
3.125e-2	1.585e-4	8.085e-5	8.449e-5	8.495e-5	8.506e-5
1.563e-2	1.701e-4	4.223e-5 1.908	2.036e-5 1.989	2.107e-5 2.004	2.118e-5 2.004
7.813e-3	1.779e-4	4.229e-5 2.008	1.089e-5 1.955	5.111e-6 1.994	5.260e-6 2.002
3.906e-3	1.813e-4	4.287e-5 2.053	1.047e-5 2.015	2.766e-6 1.977	1.280e-6 1.997
1.953e-3	1.830e-4	4.320e-5 2.069	1.042e-5 2.040	2.599e-6 2.010	6.970e-7 1.989

Table 4
Error and experimental order of convergence. Method with selection (2.20) (asymptotic selection), $\beta = 0.125$.

k	h				
	3.125e-2	1.563e-2	7.813e-3	3.906e-3	1.953e-3
3.125e-2	1.585e-4	8.297e-5	8.456e-5	8.496e-5	8.506e-5
1.563e-2	1.580e-4	4.223e-5 1.908	2.069e-5 2.004	2.109e-5 2.004	2.119e-5 2.004
7.813e-3	1.581e-4	4.033e-5 1.970	1.089e-5 1.955	5.166e-6 2.002	5.265e-6 2.002
3.906e-3	1.586e-4	3.987e-5 1.987	1.019e-5 1.985	2.766e-6 1.977	1.291e-6 2.001
1.953e-3	1.590e-4	3.982e-5 1.994	1.001e-5 1.994	2.560e-6 1.993	6.970e-7 1.989

In each entry in columns two to seven of Tables 2–4 the upper value represents the global error

$$e_{h,k} = \max \left\{ \max_{0 \leq j \leq J} |u(X_j^0, t_0) - U_j^0|, \max_{1 \leq n \leq N} \left\{ \max_{0 \leq j \leq J+1} |u(X_j^n, t_n) - U_j^n| \right\} \right\}$$

and the lower number is the experimental order s of the method as computed from

$$s = \frac{\log(e_{2h,2k}/e_{h,k})}{\log(2)}.$$

Each column and each row of the table correspond to different values of the spatial and time discretization parameter, respectively. The results in the table clearly confirm the expected second-order of convergence with every selection procedure.

In Fig. 1, we present, on a logarithmic scale, an efficiency plot where we show the error as a function of the computational time (in seconds). We build, for each selection procedure in the numerical scheme, a table with the errors corresponding to different values of parameters k and h . Then, we discover the most efficient value of r (for each selection procedure) and,

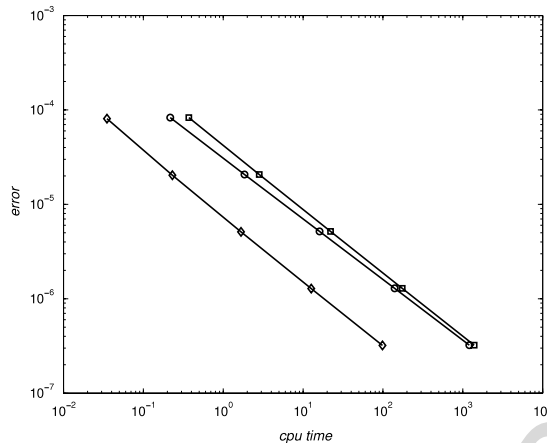


Fig. 1. Error vs. cpu-time. Selection strategy (2.21) (◇), selection strategy (2.20) (○), no selection strategy (□).

finally, we compare all the procedures in Fig. 1. We can observe that the selection procedure in which a node is eliminated at every time step shows the best behaviour.

On the other hand, we have considered a test problem which was employed in [14] in a framework in which a forest population is structured by its d.b.h. The minimum and maximum size are $x_m = 1$ and $x_M = 51$, respectively. The size-specific growth, fertility and mortality moduli are chosen as $g(x, z, t) = 7x \left(1 - \left(\frac{x}{x_M}\right)^{16}\right)$, $\alpha(x, z, t) = 0$, $\mu(x, z, t) = 0.1$. The weight function is taken as $\gamma(x) = 1$ and the external inflow function as $\Gamma(t) = R$, suitable chosen in order to satisfy the first compatibility condition. In this context, there is a constant inflow of newborns. Finally, we consider as the initial size-specific density the function

$$u_0(x) = \begin{cases} 5 + 5 \left(\frac{x-2}{2} + 1\right)^3, & x \leq 2, \\ 10 + 15 \frac{x-2}{2} \left(1 + \frac{x-2}{2}\right) + 30 \left(\frac{x-2}{2}\right)^3 \left(\frac{x-2}{2} - 2\right), & 2 < x \leq 4, \\ 5 \left(2 - \frac{x-2}{2}\right)^3 \left(2 + 3 \left(\frac{x-2}{2} - 1\right) \left(1 + 2 \left(\frac{x-2}{2} - 1\right)\right)\right), & 4 < x \leq 6, \\ 0 & x > 6. \end{cases}$$

In this case, we do not know the exact solution to the problem (1.1)–(1.4) but we know that the problem has a stable singular steady state given by

$$u^*(x) = R \frac{\exp(-\mu\varphi(x))}{g(x)}, \quad x \in [x_m, x_M],$$

where the function $\varphi(x)$ represents the time required for a tree to increase d.b.h. from x_m to x ,

$$\varphi(x) = \int_{x_0}^x \frac{d\sigma}{g(\sigma)}.$$

This problem presents a significant difficulty because the steady state has a singularity at the maximum size of the population. Similar situations have been dealt with in other related problem [8].

In Fig. 2, we present the results obtained when $T = 10$, with the first selection strategy (2.20) and discretization parameter values $k = 0.00390625$ and $h = 0.125$. On the left-hand side, we show the evolution of the total population over time and, on the right-hand side, the density distribution at $t = T$. The experiment shows that the stable steady state is reached in this time period. Clearly, the numerical method is able to obtain it.

This test shows that the best selection strategy depends on the problem we wish to solve. Its special feature means that the selection strategy that avoids useless nodes close to the maximum size exhibits the best behaviour. This is experimentally shown because when we applied the most efficient one (2.21), we also obtain this good approximation to the stable steady state but we need the discretization parameters to take values lower than $k = 0.0009765625$ and $h = 0.125$, which represents a more expensive experiment. Otherwise, oscillations or abnormal finishing of computation occur. These are only due to the type of solution we are approaching that is beyond the required hypotheses in the convergence analysis.

We could also perform other tests in which the use of other higher order numerical methods might not be suitable. However, in [5] and for an age-structured model, this lack of efficiency was shown. This is due to the fact that, in this

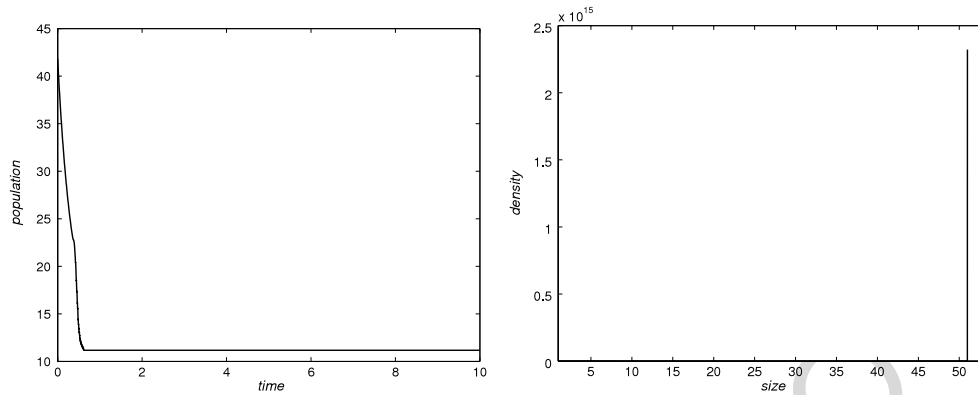


Fig. 2. Left-hand side: Evolution over time of total population computed with the first selection strategy (2.20). Right-hand side: density distribution at $t = T$.

biological framework, these kind of methods need several compatibility relationships between the initial and boundary conditions and, in reality, biological data barely satisfies the first compatibility relationship. In [5] we showed that they produce oscillations. However, characteristics methods follow perfectly the possible discontinuities in the function or in some of its derivatives.

Acknowledgement

The authors were supported in part by the Ministerio de Ciencia e Innovación (Spain), project MTM2011-25238.

References

- [1] J.A.J. Metz, E.O. Dieckmann (Eds.), *The Dynamics of Physiologically Structured Populations*, in: Springer Lecture Notes in Biomathematics, vol. 68, Springer, Heidelberg, 1986.
- [2] G.F. Webb, *Theory of Nonlinear Age-Dependent Population Dynamics*, Marcel Dekker, New York, 1985.
- [3] M. Iannelli, *Mathematical Theory of Age-Structured Population Dynamics*, in: Applied Mathematics Monographs, C.N.R., Giardini Editori e Stampatori, Pisa, 1994.
- [4] J.M. Cushing, *An Introduction to Structured Population Dynamics*, in: CMB-NSF Regional Conference Series in Applied Mathematics, SIAM, 1998.
- [5] L.M. Abia, O. Angulo, J.C. López-Marcos, Age-structured population dynamics models and their numerical solutions, *Ecol. Model.* 188 (2005) 112–136.
- [6] L.M. Abia, O. Angulo, J.C. López-Marcos, Size-structured population dynamics models and their numerical solutions, *Discrete Contin. Dyn. Syst. Ser. B* 4 (2004) 1203–1222.
- [7] M. Adimy, O. Angulo, F. Crauste, J.C. López-Marcos, Numerical integration of a mathematical model of hematopoietic stem cell dynamics, *Comput. Math. Appl.* 56 (2008) 594–606.
- [8] O. Angulo, J.C. López-Marcos, M.A. López-Marcos, Numerical approximation of singular asymptotic states for a size-structured population model with a dynamical resource, *Math. Comput. Modelling* 54 (2011) 1693–1698.
- [9] O. Angulo, J.C. López-Marcos, M.A. Bees, Mass structured systems with boundary delay: oscillations and the effect of selective predation, *J. Nonlinear Sci.* 22 (2012) 961–984.
- [10] O. Angulo, J.C. López-Marcos, M.A. López-Marcos, A semi-Lagrangian method for a cell population model in a dynamical environment, *Math. Comput. Modelling* 57 (2013) 1860–1866.
- [11] O. Angulo, J.C. López-Marcos, M.A. López-Marcos, J. Martínez-Rodríguez, Numerical analysis of a population model of marine invertebrates with different life stages, *Commun. Nonlinear Sci. Numer. Simul.* 18 (2013) 2153–2163.
- [12] T. Kohyama, Size-structured multi-species model of rain forest trees, *Funct. Ecol.* 6 (1992) 206–212.
- [13] M.A. Zavala, R. Bravo de la Parra, A mechanistic model of tree competition and facilitation for Mediterranean forests: scaling from leaf physiology to stand dynamics, *Ecol. Mod.* 188 (2005) 76–92.
- [14] M.A. Zavala, O. Angulo, R. Bravo de la Parra, J.C. López-Marcos, An analytical model of stand dynamics as a function of tree growth, mortality and recruitment: the shade tolerance-stand structure hypothesis revisited, *J. Theoret. Biol.* 244 (2007) 440–450.
- [15] J.M. Cushing, The dynamics of hierarchical age-structured populations, *J. Math. Biol.* 32 (1994) 705–729.
- [16] A. Calsina, J. Saldaña, Asymptotic behaviour of a model of hierarchically structured population dynamics, *J. Math. Biol.* 35 (1997) 967–987.
- [17] E.A. Kraev, Existence and uniqueness for height structured hierarchical population models, *Nat. Resour. Model.* 14 (2001) 45–70.
- [18] A.S. Ackleh, K. Ito, Measure-valued solutions for a hierarchically size-structured population, *J. Differential Equations* 217 (2005) 431–455.
- [19] A.S. Ackleh, K. Ito, A quasilinear hierarchical size-structured model: well-posedness and approximation, *Appl. Math. Optim.* 51 (2005) 35–59.
- [20] J. Shen, C.-W. Shu, M. Zhang, High resolution schemes for a hierarchical size-structured model, *SIAM J. Numer. Anal.* 45 (2007) 352–370.
- [21] A. Calsina, J. Saldaña, A model of physiologically structured population dynamics with a nonlinear individual growth rate, *J. Math. Biol.* 33 (1995) 335–364.
- [22] O. Angulo, A. Durán, J.C. López-Marcos, Numerical study of size-structured population models: a case of *Gambusia affinis*, *C. R. Biol.* 328 (2005) 387–402.
- [23] A.J. Fabens, Properties and fitting of the von Bertalanffy growth curve, *Growth* 29 (1965) 265–289.
- [24] D. Sulsky, Numerical solution of structured population models II. Mass structure, *J. Math. Biol.* 32 (1994) 491–514.
- [25] O. Angulo, J.C. López-Marcos, Numerical integration of fully nonlinear size-structured population models, *Appl. Numer. Math.* 50 (2004) 291–327.
- [26] J.C. López-Marcos, J.M. Sanz-Serna, Stability and convergence in numerical analysis III: linear investigation of nonlinear stability, *IMA J. Numer. Anal.* 8 (1988) 71–84.